Radiative Transfer Equation and Solutions

Chapter · January 2017

DOI: 10.1007/978-3-319-32003-8_56-1

2 authors:


J. M. Zhao
Harbin Institute of Technology


L. H. Liu
Harbin Institute of Technology

Radiative Transfer Equation and Solutions

J.M. Zhao and L.H. Liu

School of energy science and engineering, Harbin Institute of Technology, China
e-mail: jmzhao@hit.edu.cn (J.M. Zhao), lhliu@hit.edu.cn (L.H. Liu)

Abstract

Radiative transfer equation (RTE) is the governing equation of radiation propagation in participating media, which plays a central role in the analysis of radiative transfer in gases, semitransparent liquids and solids, porous materials and particulate media, and is important in many scientific and engineering disciplines. There are different forms of RTEs that are suitable for different applications, including the RTE under different coordinates systems, the transformed RTE being numerically more stable, the RTE for refractive media, etc. This chapter gives a comprehensive overview and introduction of the different forms of RTEs. Furthermore, several fundamental numerical methods for solving RTEs are introduced with the focus on the deterministic methods, such as the spherical harmonics method, discrete ordinates method, finite volume method and finite element method. The understanding of the numerical errors for solving the RTEs, including their origin and effects on numerical results, and the related accuracy improvement strategies are reviewed and discussed.

Contents

1. Introduction

Radiative transfer equation is the governing equation of radiation propagation in participating media, which describes the general balance of radiative energy transport in the participating media taking into account the interactions of attenuation and augmentation by absorption, scattering and emission processes (Howell et al. 2016; Modest 2013). The equations of radiative transfer play a central role in the analysis of radiative transfer in gases, semitransparent liquids and solids, porous materials and particulate media, which are important in many scientific and engineering disciplines, such as combustion systems (Viskanta and Mengüç 1987; Modest and Haworth 2016), rockets (Simmons 2000), atmospheric radiation (Liou 2002), remote sensing, astrophysics, non-contact temperature field measurement (Zhou et al. 2005), optical tomography (Klose et al. 2002), photo-bioreactors (Pilon et al. 2011; Berberoglu et al. 2007), and solar energy harvesting (Benoit et al. 2016; Agrafiotis et al. 2007; Mahian et al. 2013), among others.

The classical equation of radiative transfer is a first order integral-differential equation describing radiative energy transport in media with uniform refractive index, i.e., light beam propagates through straight lines in the media. It has been widely applied to radiative transfer analysis in scientific and engineering problems and demonstrated to be a reliable theory for engineering applications. There are many variant forms of radiative transfer equations. For example, in order for convenience of solution for specific problems, the equations of radiative transfer are usually formulated under different coordinate systems and shown in different forms, such as Lagrange form in ray path coordinate and Eulerian forms in common orthogonal coordinate systems, such as Cartesian coordinate system and cylindrical coordinate system, etc. Furthermore, the traditional form of radiative transfer equations, namely, the first order integral-differential equation, can be transformed to second order forms to improve stability for numerical solution, such as the even-parity formulation of radiative transfer equation (Song and Park 1992) and the second order radiative transfer equations (Zhao et al. 2013; Zhao and Liu 2007a). However, due to the structural characteristics of a material or a possible temperature/pressure dependency, the refractive index of a medium may be a function of spatial position. Some examples of participating media with gradient refractive index distribution are earth's (or other planets') atmosphere, the ocean water, the hot air/gas of a flame, and artificial materials, such as graded index lens, graded index optical fiber, etc. In such cases, the classical equation of radiative transfer has to be extended to take into account the effect of curved ray path, resulting in the equation of radiative transfer in refractive media (Liu and Tan 2006). Radiative transfer in graded index media has attracted the interest of many researchers, some recent works include Refs. (Asllanaj and Fumeron 2010; Wu and Hou 2012; Zhang et al. 2012; Hou et al. 2015; Chai et al. 2015; Huang et al. 2016), to name a few.

Numerical simulation is crucial to analyze radiative transfer in real applications, since analytical solutions exist only for a few simple cases due to the mathematical complexity of radiative transfer equation and the complex configuration of the problems. However, numerical simulation of radiative transfer in participating media is usually time consuming and requires considerable effort due to the complexity and the high dimensionality of radiative transfer process, which contains additional dimensions of one frequency and two angular dimensions besides the common three spatial dimensions. Hence efficient and accurate numerical methods are very important for most practical applications. Many efforts have been devoted to devise effective methods for the analysis of radiative transfer in participating media. Until recently, many numerical methods have been developed for the solution of radiative transfer equation. Generally, the methods can be classified into two groups, the first group is based on stochastic simulation, which includes various implementation of Monte Carlo methods (MCM) (Howell 1968; Farmer and Howell 1994; Siegel and Howell 2002), the DESOR method (Zhou and Cheng 2004), and the second group is the deterministic methods, such as spherical harmonics method (or P_N approximation)(Mengüç and Viskanta 1985; Larsen et al. 2002), discrete ordinate methods (DOM) (Carlson and Lathrop 1965; Fiveland 1988; Coelho 2002a), finite volume method (FVM) (Raithby and Chui 1990; Chai and Lee 1994; Murthy and Mathur 1998; Asllanaj and Fumeron 2010), finite element method (FEM) (Liu et al. 2008), radiation element method (Maruyama 1993), spectral element method (Zhao and Liu 2006), spectral methods (Li et al. 2008) and meshless methods (Sadat 2006; Liu and Tan 2007), to name a few. A review of numerical methods for solving the RTE refers to the textbook by Modest (Modest 2013).

As being approximate methods, all numerical methods suffer several kinds of numerical errors. The MC method suffers from statistic errors. The DOM, FVM and FEM suffer from space and angular discretization errors. The significance of numerical errors is problem dependent. It will add unphysical features to the solution to make the solution difficult to be interpreted and may sometimes totally spoil the solution. Hence the knowledge of the origin and characteristics of numerical errors is important, which can help to interpret the results of numerical simulation and to design strategies to reduce or eliminate the errors. It has been known for decades that DOM method suffers two kinds of numerical errors, i.e., false scattering and ray effects, and several strategies have been proposed to reduce these errors (Chai et al. 1993). The FVM can be considered a DOM with a special angular quadrature scheme, and FEM and many other methods are based on the discrete ordinates equations. Thus the false scattering and ray effects are two general kinds of numerical errors, which needs to be thoroughly understood. Recently, Hunter and Guo (Hunter and Guo 2015) gave a comprehensive analysis on the numerical errors on solution of RTE.

In this chapter, the classical radiative transfer equation and several variant forms of radiative transfer equation, different solution techniques for the radiative transfer equations, numerical errors on the solution of radiative transfer equation and the related improvement strategies are presented and discussed. The chapter is organized as follows. Firstly, the classical radiative transfer equation and variant forms of radiative transfer equation are presented in Section 2. Then, the different solution techniques for the radiative transfer equation are introduced in Section 3. Finally, the numerical errors on the solution of radiative transfer equation and the related improvement strategies are presented in Section 4.

2. Radiative Transfer Equation

In this section, the governing equations of radiative transfer, including the classic radiative transfer equation, the radiative transfer equation in refractive media, and the different variant forms of the radiative transfer equations are introduced.

2.1. The classical radiative transfer equation (RTE)

The classical equation of radiative transfer describes the balance of radiative energy transport in absorbing, emitting and scattering media with uniform refractive index distribution. Generally, the radiative power of a light beam in the medium is a function of wavelength λ ($\mu\mathrm{m}$), transfer direction $\mathbf{\Omega}$ and spatial location $\mathbf{r}$, which is described using the physical quantity of radiative intensity $I_\lambda(\mathbf{r}, \mathbf{\Omega})$. It has unit $\mathrm{W/(m^2 \mu m\, sr)}$, denoting the transferred radiative power per unit cross-section area along the transfer direction, per wavelength and per solid angle. The RTE is a governing equation of radiative intensity $I_\lambda(\mathbf{r},\mathbf{\Omega})$. In the following, the RTE in different coordinate system, the energy relations and numerical properties of RTE are presented. The photon description of light is used throughrout the chapter as it is commonly applied for phenomenological derivation of the RTE. It is noted that light is indeed electromagnetic wave and the rigorous description of radiative transfer should be based on Maxwell equations.

2.1.1. Ray path coordinate system formulation

Ray path coordinate is the natural coordinate system for light transfer. Here the RTE is formulated in the one-dimensional Lagrangian ray path coordinate at first. The Lagrangian form of RTE is the physically clearest, in the simplest mathematical form and considered to be the most general formulation such that the RTE under other different coordinate systems can be derived just by expressing the stream operator under the system.

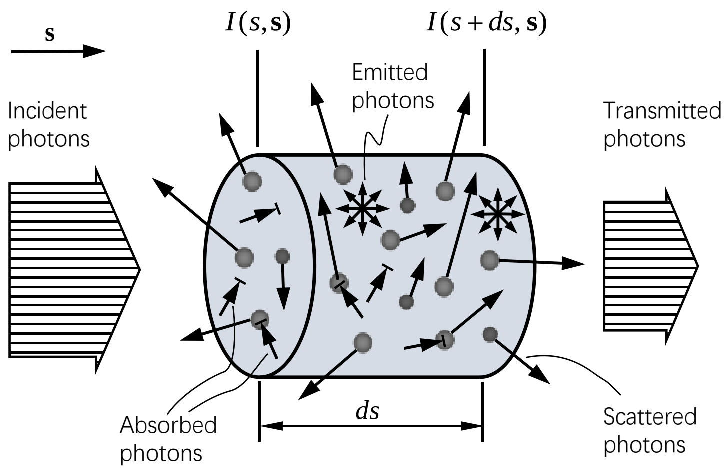

Fig. 1. Schematic of light transport in participating medium. The photon beam is attenuated by absorption and out-scattering and augmented by emission and in-scattering processes.

A control volume in cylinder shape along the ray path between s and $s+ds$ is considered as shown in Fig. 1. A light beam enters the left surface at s, and exits at $s+ds$. The end surface of the cylinder is perpendicular to the ray transfer direction $\mathbf{s}$ with an area of dA. The radiative intensity along the ray path direction can be expressed as $I_\lambda(s,\mathbf{s})$. At the same location, the radiative intensity of any other direction $\mathbf{\Omega}$ can be expressed as $I_\lambda(s,\mathbf{\Omega})$. When the light beam (photons) moves from location s to $s+ds$, the balance of spectral radiative power Q_λ (W) can be expressed as follows.

$$\Delta Q_\lambda = \underbrace{\left(\Delta Q_{\lambda,\text{abs}} + \Delta Q_{\lambda,\text{out-scatt}}\right)}_{\text{Attenuation}} + \underbrace{\left(\Delta Q_{\lambda,\text{emit}} + \Delta Q_{\lambda,\text{in-scatt}}\right)}_{\text{Augmentation}} \tag{1.1}$$

where ΔQ_λ denotes the variation of spectral radiative power along the differential ray path ds, which can be calculated by definition as $\Delta Q_\lambda = \left[I_\lambda(s+ds,\mathbf{s}) - I_\lambda(s,\mathbf{s})\right]dAd\Omega$, $d\Omega$ is a differential solid angle, the four terms at right hand side indicate the contributions of the basic interaction mechanisms in participating media, namely, absorption ($\Delta Q_{\lambda,\text{abs}}$), scattering ($\Delta Q_{\lambda,\text{out-scatt}}$ and $\Delta Q_{\lambda,\text{in-scatt}}$) and emission processes ($\Delta Q_{\lambda,\text{emit}}$). Absorption process transfers the radiative power to kinetic energy of heat carriers (e.g. electrons and phonons), which only attenuates the radiative power. Thermal emission process only augments the radiative power. As for the scattering process, it can both attenuate and augment the radiative power depending on whether it is the scattering of the current light beam $I_\lambda(s,\mathbf{s})$ to other directions, i.e., the out-scattering process, or the scattering of light beam of other direction $I_\lambda(s,\mathbf{\Omega})$ to current transfer direction $\mathbf{s}$, i.e., the in-scattering process.

The attenuated radiative power in the control volume is proportional to the incident radiative power, which for the processes of absorption and out-scattering can be established respectively as

$$\Delta Q_{\lambda,\text{abs}} = -\kappa_{a,\lambda} I_\lambda(s,\mathbf{s}) ds dA d\Omega,\ \ \Delta Q_{\lambda,\text{out-scatt}} = -\kappa_{s,\lambda} I_\lambda(s,\mathbf{s}) ds dA d\Omega \tag{1.2}$$

where $\kappa_{a,\lambda}$ (m^{-1}) and $\kappa_{s,\lambda}$ (m^{-1}) are the spectral *absorption coefficient* and *scattering coefficient*, respectively. The emitted radiative power in the control volume is established based on the black body radiative intensity as

$$\Delta Q_{\lambda,\text{emit}} = \kappa_{a,\lambda} I_{b,\lambda}[T(s)] ds dA d\Omega \tag{1.3}$$

in which Kirchhoff's law of thermal radiation is applied, $\kappa_{a,\lambda} ds$ can be viewed as the emissivity of the layer of medium with thickness ds, $I_{b,\lambda}$ is the black body spectral radiative intensity. For a black body in a transparent medium with refractive index n_λ, $I_{b,\lambda}$ is calculated from (Modest 2013)

$$I_{b,\lambda} = n_\lambda^2 I_{b,\lambda}^0 = \frac{2hc^2 n_\lambda^2}{\lambda^5\left(e^{hc/\lambda k_B T} - 1\right)} \tag{1.4}$$

where $I_{b,\lambda}^0$ is the radiative intensity of black body in vacuum, $c = 2.998\times10^8$ (m/s) is vacuum light speed, $h = 6.626\times10^{-34}$ (J s) is the Planck's constant, $k_B = 1.3807\times10^{-23}$ (J/K) is the Boltzmann's constant. Note that the wavelength λ denotes vacuum wavelength throughout this text.

The scattering process generally changes the direction of incident photons. This angular redistribution of incident photons by scattering process is described by the *scattering phase function*, which expresses the ratio of radiative power scattered to each direction per solid angle. By definition, the scattering phase function $\Phi_\lambda(\cos\Theta)$ (sr^{-1}) must satisfy scattering energy conservation, which is often called normalization relation and written as

$$\frac{1}{4\pi}\int_{4\pi}\Phi_\lambda(\cos\Theta)d\Omega = 1 \tag{1.5}$$

where $\cos\Theta = \mathbf{\Omega}'\bullet\mathbf{\Omega}$ is the cosine of the angle between incident ($\mathbf{\Omega}'$) and scattering direction ($\mathbf{\Omega}$). For a light beam with radiative intensity $I_\lambda(\mathbf{\Omega}', s)$ incident on a differential control volume with volume dV , the total scattered radiative power by the scatterers in the control volume is $\kappa_{s,\lambda}I_\lambda(\mathbf{\Omega}', s)dVd\Omega'$ according to Eq. (1.2), where $d\Omega'$ is a differential solid angle related to the incident beam of direction $\mathbf{\Omega}'$. Then the scattered power from an arbitrary incident direction $\mathbf{\Omega}'$ to the current transfer direction $\mathbf{s}$ is $\kappa_{s,\lambda}I_\lambda(s, \mathbf{\Omega}')\frac{1}{4\pi}\Phi_\lambda(\mathbf{\Omega}'\bullet\mathbf{s})dVd\Omega'd\Omega$. The total in-scattering radiative power augmentation from all directions can then be calculated by integration as

$$\Delta Q_{\lambda,\text{in-scatt}} = \frac{\kappa_{s,\lambda}}{4\pi}\int_{4\pi} I_\lambda(s, \mathbf{\Omega}')\Phi_\lambda(\mathbf{\Omega}'\bullet\mathbf{s})d\Omega' ds dA d\Omega \tag{1.6}$$

By substitution of Eqs. (1.3), (1.2) and (1.6) into Eq. (1.1), the Lagrangian form of RTE can be obtained as

$$\frac{\mathrm{d}I_\lambda(s,\mathbf{s})}{\mathrm{d}s} + \beta_\lambda I_\lambda(s,\mathbf{s}) = \kappa_{a,\lambda}I_{b,\lambda}[T(s)] + \frac{\kappa_{s,\lambda}}{4\pi}\int_{4\pi} I_\lambda(s,\mathbf{\Omega}')\Phi_\lambda(\mathbf{\Omega}'\bullet\mathbf{s})\mathrm{d}\Omega' \tag{1.7}$$

where $\beta_\lambda = (\kappa_{a,\lambda} + \kappa_{s,\lambda})$ is the extinction coefficient. If the ray coordinate is not moved with beam propagation, namely, Eulerian frame is used, the radiative intensity will be function of time t and the fixed ray coordinate s , and can be expressed as $I_\lambda(s, t, \mathbf{s})$. In this case, the Lagrangian stream operator $\mathrm{d}/\mathrm{d}s$ can be expanded as

$$\frac{\mathrm{d}}{\mathrm{d}s} = \frac{\partial}{\partial s} + \frac{\partial}{\partial t}\frac{dt}{ds} = \frac{\partial}{\partial s} + \frac{n_\lambda}{c}\frac{\partial}{\partial t} \tag{1.8}$$

where c is the light speed in vacuum. Using Eq. (1.8), the RTE can be expressed in Eulerian form as

$$\begin{aligned}\frac{n_\lambda}{c}\frac{\partial I_\lambda(s,t,\mathbf{s})}{\partial t} &+ \frac{\partial I_\lambda(s,t,\mathbf{s})}{\partial s} + \beta_\lambda I_\lambda(s,t,\mathbf{s}) \\ &= \kappa_{a,\lambda}I_{b,\lambda}[T(s)] + \frac{\kappa_{s,\lambda}}{4\pi}\int_{4\pi} I_\lambda(s,t,\mathbf{\Omega}')\Phi_\lambda(\mathbf{\Omega}'\bullet\mathbf{s})\mathrm{d}\Omega'\end{aligned} \tag{1.9}$$

Equations (1.7) and (1.9) are the basic form of RTEs in uniform refractive index media. As can be seen, for steady state radiative transfer, Eqs. (1.7) and (1.9) are the same. Equation (1.9) is specially useful for transient radiative transfer analysis. The RTEs in other coordinate systems can be derived by simply expressing the stream operator in the coordinate system. In the following, only steady state RTE is considered unless otherwise mentioned.

2.1.2. Cartesian coordinate system formulation

In Cartesian coordinate system, radiative intensity is expressed as $I_\lambda(s(x,y,z),\mathbf{\Omega})$, hence,

$$\frac{\mathrm{d}I}{\mathrm{d}s}=\frac{\mathrm{d}x}{\mathrm{d}s}\frac{\partial I}{\partial x}+\frac{\mathrm{d}y}{\mathrm{d}s}\frac{\partial I}{\partial y}+\frac{\mathrm{d}z}{\mathrm{d}s}\frac{\partial I}{\partial z} \tag{1.10}$$

Considering $\mathrm{d}s$ as the arc length along a curve, the coordinates transformation coefficients $\mathrm{d}x/\mathrm{d}s$, $\mathrm{d}y/\mathrm{d}s$ and $\mathrm{d}z/\mathrm{d}s$ are the direction cosines of the transport direction $\mathbf{\Omega}=\mu\mathbf{i}+\eta\mathbf{j}+\xi\mathbf{k}$. As such, Eq. (1.10) can be written as

$$\frac{\mathrm{d}I}{\mathrm{d}s}=\mu\frac{\partial I}{\partial x}+\eta\frac{\partial I}{\partial y}+\xi\frac{\partial I}{\partial z}=\mathbf{\Omega}\bullet\nabla I \tag{1.11}$$

The RTE in Cartesian coordinate system can then be written as

$$\mathbf{\Omega}\bullet\nabla I_\lambda(\mathbf{r},\mathbf{\Omega})+\beta_\lambda I_\lambda(\mathbf{r},\mathbf{\Omega})=\kappa_{a,\lambda}I_{b,\lambda}[T(\mathbf{r})]+\frac{\kappa_{s,\lambda}}{4\pi}\int_{4\pi}I_\lambda(\mathbf{r},\mathbf{\Omega}')\Phi_\lambda(\mathbf{\Omega}'\bullet\mathbf{\Omega})\mathrm{d}\Omega' \tag{1.12}$$

where $\mathbf{r}=x\mathbf{i}+y\mathbf{j}+z\mathbf{k}$ is the spatial location vector.

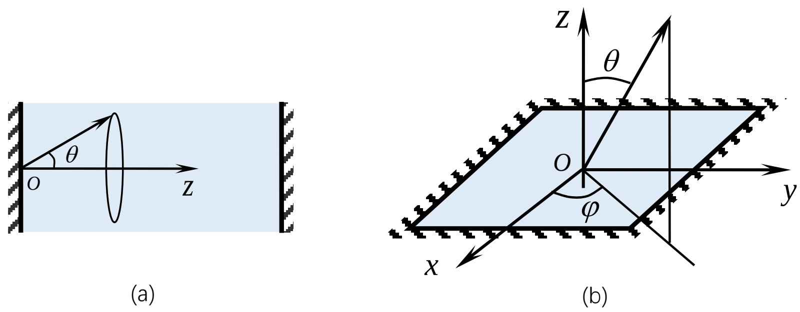

Fig. 2. 1D and 2D Cartesian system with variable defined to formulate the RTE. (a) 1D and (b) 2D.

For 1D and 2D cases, the equation can be simplified by employing the symmetries of radiative intensity distribution, i.e., the axisymmetric around z-axis for 1D and mirror symmetry about z-axis for 2D case as shown in Fig. 2. The 1D RTE can be written as

$$\xi\frac{\mathrm{d}I_\lambda(\mathrm{z},\xi)}{\mathrm{d}z}+\beta_\lambda I_\lambda(\mathrm{z},\xi)=\kappa_{a,\lambda}I_{b,\lambda}[T(z)]+\int_{-1}^{1}I(\mathrm{z},\xi')\Phi_{1,\lambda}(\xi',\xi)\,\mathrm{d}\,\xi' \tag{1.13}$$

where $\xi=\cos\theta$, $\Phi_{1,\lambda}(\xi',\xi)=\frac{1}{2\pi}\int_0^{2\pi}\Phi(\mathbf{\Omega}'\bullet\mathbf{\Omega})\,\mathrm{d}\,\varphi$ is the 1D scattering phase function. If the scattering phase function can be expanded in Legendre Polynomials P_m as

$$\Phi(\mathbf{\Omega}'\bullet\mathbf{\Omega}) = \Phi(\cos\Theta) = 1 + \sum_{m=1}^{M} A_m P_m(\cos\Theta) \tag{1.14}$$

where A_m is the *m*-th order expansion coefficient. Then the 1D scattering phase function can be expressed as (Modest 2013)

$$\Phi_{1,\lambda}(\xi',\xi) = 1 + \sum_{m=1}^{M} A_m P_m(\xi') P_m(\xi) \tag{1.15}$$

For 2D case, the mirror symmetry indicates $I(\mathbf{\Omega},\mathbf{r}) = I(\bar{\mathbf{\Omega}},\mathbf{r})$, where $\bar{\mathbf{\Omega}}_m = [\mu,\eta,-\xi]$, hence the RTE can be written as (Zhao et al. 2013)

$$\mu\frac{\partial I_\lambda}{\partial x} + \eta\frac{\partial I_\lambda}{\partial y} + \beta_\lambda I_\lambda = \kappa_{a,\lambda} I_{b,\lambda} + \frac{\kappa_{s,\lambda}}{4\pi}\int_{2\pi} I_\lambda(\mathbf{r},\mathbf{\Omega}')\Phi_{2,\lambda}(\mathbf{\Omega}'\bullet\mathbf{\Omega})\mathrm{d}\Omega' \tag{1.16}$$

Where $\Phi_{2,\lambda}(\mathbf{\Omega}'\bullet\mathbf{\Omega}) = \Phi_\lambda(\mathbf{\Omega}'\bullet\mathbf{\Omega}) + \Phi_\lambda(\bar{\mathbf{\Omega}}'\bullet\mathbf{\Omega})$ is the 2D scattering phase function, and the angular quadrature is only over half solid angular space at $\theta \in [0, \pi/2]$.

2.1.3. RTE in other coordinate systems

Besides the Cartesian coordinate system, cylindrical and spherical coordinate system are the other two commonly used orthogonal coordinate systems. Here the RTE in these coordinate systems are presented. Currently, two types of cylindrical coordinates system (*ρ*-*Ψ*-*z*-*θ*-*φ*) were proposed for radiative transfer analysis in literatures, whose definitions are shown in Fig. 3. The Type I cylindrical coordinate system is the traditional one (Modest 2013), and the Type II cylindrical coordinate system is a relatively new one proposed recently (Zhang et al. 2010). The difference between these two systems lies in the definition of local angular variables, i.e., the zenith angle θ and azimuthal angle φ. By definition, the optical plane of reflection or refraction at the cylindrical interfaces coincides with the iso-surface of azimuthal angle φ in the Type II system, hence it facilitates the treatment of reflection/refraction at the cylindrical interfaces/boundaries.

For the Type I cylindrical coordinates system [Fig. 3(a)], the stream operator d/ds can be expanded as (Modest 2013)

$$\begin{aligned} \frac{d}{ds} &= \frac{d\rho}{ds}\frac{\partial}{\partial\rho} + \frac{d\Psi}{ds}\frac{\partial}{\partial\Psi} + \frac{dz}{ds}\frac{\partial}{\partial z} + \frac{d\theta}{ds}\frac{\partial}{\partial\theta} + \frac{d\varphi}{ds}\frac{\partial}{\partial\varphi} \\ &= \mathbf{\Omega}\bullet\nabla_{\mathrm{I}} - \frac{\eta}{\rho}\frac{\partial}{\partial\varphi} \end{aligned} \tag{1.17}$$

where $\mathbf{\Omega} = \mu\mathbf{e}_\rho + \eta\mathbf{e}_\Psi + \xi\mathbf{e}_z$ is the local direction vector of the beam, $\mu = \sin\theta\cos\varphi$, $\eta = \sin\theta\sin\varphi$, $\xi = \cos\theta$, $\mathbf{e}_\rho$, $\mathbf{e}_\Psi$ and $\mathbf{e}_z$ are the unit coordinate vectors, $\nabla_{\mathrm{I}} = \mathbf{e}_\rho\partial/\partial\rho + \mathbf{e}_\Psi\rho^{-1}\partial/\partial\Psi + \mathbf{e}_z\partial/\partial z$ is the gradient operator in the Type I Cylindrical coordinate system. Hence the RTE in the Type I cylindrical coordinate system can be written as

$$\mathbf{\Omega}\bullet\nabla I_{\lambda}-\frac{\eta}{\rho}\frac{\partial I_{\lambda}}{\partial\varphi}+\beta_{\lambda}I_{\lambda}=\kappa_{a,\lambda}I_{b,\lambda}+\frac{\kappa_{s,\lambda}}{4\pi}\int_{4\pi}I_{\lambda}(\mathbf{r},\mathbf{\Omega}')\Phi_{\lambda}(\mathbf{\Omega}'\bullet\mathbf{\Omega})\mathrm{d}\Omega' \tag{1.18}$$

This is in non-conservative form, and it can be further rewritten in conservative form as

$$\mathbf{\Omega}\bullet\tilde{\nabla}_{\mathrm{I}}I_{\lambda}-\frac{1}{\rho}\frac{\partial\eta I_{\lambda}}{\partial\varphi}+\beta_{\lambda}I_{\lambda}=\kappa_{a,\lambda}I_{b,\lambda}+\frac{\kappa_{s,\lambda}}{4\pi}\int_{4\pi}I_{\lambda}(\mathbf{r},\mathbf{\Omega}')\Phi_{\lambda}(\mathbf{\Omega}'\bullet\mathbf{\Omega})\mathrm{d}\Omega' \tag{1.19}$$

where $\tilde{\nabla}_{\mathrm{I}}(\bullet)=\mathbf{e}_{\rho}\rho^{-1}\partial(\rho\,\bullet)/\partial\rho+\mathbf{e}_{\Psi}\rho^{-1}\partial(\bullet)/\partial\Psi+\mathbf{e}_{z}\rho^{-1}\partial(\bullet)/\partial z$ is a modified gradient operator in the Type I cylindrical coordinate system.

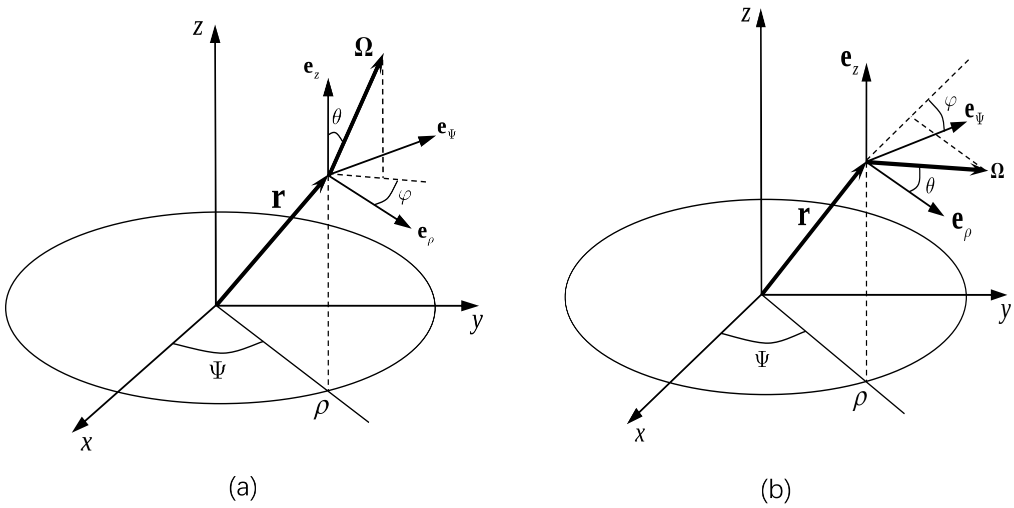

Fig. 3. Definition of the cylindrical coordinate system. (a) Type I and (b) Type II.

For the Type II cylindrical coordinates system [Fig. 3(b)], the stream operator can be expanded as (Zhang et al. 2010; Zhao et al. 2012b)

$$\frac{d}{ds}=\mathbf{\Omega}\bullet\nabla_{\mathrm{II}}-\mu\frac{\cos\varphi}{\rho}\frac{\partial}{\partial\theta}+\xi\frac{\sin\varphi\cos\varphi}{\rho}\frac{\partial}{\partial\varphi} \tag{1.20}$$

where $\mathbf{\Omega}=\mu\mathbf{e}_{\Psi}+\eta\mathbf{e}_{z}+\xi\mathbf{e}_{\rho}$ is the local direction vector of the beam, and the gradient operator is given as $\nabla_{\mathrm{II}}=\mathbf{e}_{\Psi}\rho^{-1}\partial/\partial\Psi+\mathbf{e}_{z}\partial/\partial z+\mathbf{e}_{\rho}\partial/\partial\rho$. The RTE in the Type II cylindrical coordinate system can thus be written as

$$\begin{aligned}&\mathbf{\Omega}\bullet\nabla_{\mathrm{II}}I_\lambda-\mu\frac{\cos\varphi}{\rho}\frac{\partial I_\lambda}{\partial\theta}+\xi\frac{\sin\varphi\cos\varphi}{\rho}\frac{\partial I_\lambda}{\partial\varphi}+\beta_\lambda I_\lambda\\&=\kappa_{a,\lambda}I_{b,\lambda}+\frac{\kappa_{s,\lambda}}{4\pi}\int_{4\pi}I_\lambda(\mathbf{r},\mathbf{\Omega}')\Phi_\lambda(\mathbf{\Omega}'\bullet\mathbf{\Omega})\mathrm{d}\Omega'\end{aligned}\tag{1.21}$$

This is in non-conservative form, and it can be further rewritten in conservative form as

$$\begin{aligned}&\mathbf{\Omega}\bullet\tilde{\nabla}_{\mathrm{II}}I_\lambda-\frac{1}{\rho\sin\theta}\frac{\partial}{\partial\theta}\left[\mu^2I_\lambda\right]+\frac{1}{\rho}\frac{\partial}{\partial\varphi}\left[\xi\sin\varphi\cos\varphi I_\lambda\right]+\beta_\lambda I_\lambda\\&=\kappa_{a,\lambda}I_{b,\lambda}+\frac{\kappa_{s,\lambda}}{4\pi}\int_{4\pi}I_\lambda(\mathbf{r},\mathbf{\Omega}')\Phi_\lambda(\mathbf{\Omega}'\bullet\mathbf{\Omega})\mathrm{d}\Omega'\end{aligned}\tag{1.22}$$

where $\tilde{\nabla}_{\mathrm{II}}\ \bullet\ =\mathbf{e}_\Psi\rho^{-1}\partial\ \bullet\ /\partial\Psi+\mathbf{e}_z\partial\ \bullet\ /\partial z+\mathbf{e}_\rho\rho^{-1}\partial\ \rho\bullet\ /\partial\rho$ is a modified gradient operator.

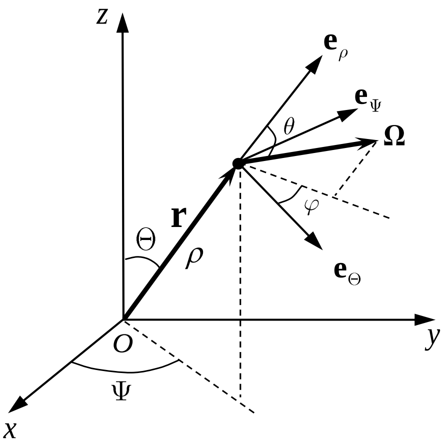

Fig. 4. Definition of the spherical coordinate system.

For the spherical coordinate system (Θ - Ψ - ρ - θ - φ) defined in Fig. 4, the stream operator can be expanded as (Liu et al. 2008)

$$\begin{aligned}\frac{d}{ds}&=\frac{d\Theta}{ds}\frac{\partial}{\partial\Theta}+\frac{d\Psi}{ds}\frac{\partial}{\partial\Psi}+\frac{d\rho}{ds}\frac{\partial}{\partial\rho}+\frac{d\theta}{ds}\frac{\partial}{\partial\theta}+\frac{d\varphi}{ds}\frac{\partial}{\partial\varphi}\\&=\mathbf{\Omega}\bullet\nabla-\frac{\sin\theta}{\rho}\frac{\partial}{\partial\theta}-\frac{\eta\cot\Theta}{\rho}\frac{\partial}{\partial\varphi}\end{aligned}\tag{1.23}$$

where $\mathbf{\Omega}=\mu\mathbf{e}_\Theta+\eta\mathbf{e}_\Psi+\xi\mathbf{e}_\rho$ is the local direction vector of the beam, the gradient operator is defined as $\nabla=\mathbf{e}_\Theta\rho^{-1}\partial/\partial\Theta+\mathbf{e}_\Psi\ \rho\sin\Theta\ ^{-1}\partial/\partial\Psi+\mathbf{e}_\rho\partial/\partial\rho$. The RTE in the spherical coordinate system can be obtained in the non-conservative form as

$$\begin{aligned}&\mathbf{\Omega}\bullet\nabla I_\lambda-\frac{\sin\theta}{\rho}\frac{\partial I_\lambda}{\partial\theta}-\frac{\eta\cot\Theta}{\rho}\frac{\partial I_\lambda}{\partial\varphi}+\beta_\lambda I_\lambda\\&=\kappa_{a,\lambda}I_{b,\lambda}+\frac{\kappa_{s,\lambda}}{4\pi}\int_{4\pi}I_\lambda(\mathbf{r},\mathbf{\Omega}')\Phi_\lambda(\mathbf{\Omega}'\bullet\mathbf{\Omega})\mathrm{d}\Omega'\end{aligned}\tag{1.24}$$

and in the conservative form as

$$\begin{aligned}&\mathbf{\Omega}\bullet\tilde{\nabla}I_\lambda-\frac{1}{\rho\sin\theta}\frac{\partial(1-\xi^2)I_\lambda}{\partial\theta}-\frac{\cot\Theta}{\rho}\frac{\partial\eta I_\lambda}{\partial\varphi}+\beta_\lambda I_\lambda\\&=\kappa_{a,\lambda}I_{b,\lambda}+\frac{\kappa_{s,\lambda}}{4\pi}\int_{4\pi}I_\lambda(\mathbf{r},\mathbf{\Omega}')\Phi_\lambda(\mathbf{\Omega}'\bullet\mathbf{\Omega})\mathrm{d}\Omega'\end{aligned}\tag{1.25}$$

where $\tilde{\nabla}(\bullet)=\mathbf{e}_\Theta(\rho\sin\Theta)^{-1}\partial(\sin\Theta\,\bullet)/\partial\Theta+\mathbf{e}_\Psi(\rho\sin\Theta)^{-1}\partial/\partial\Psi+\mathbf{e}_\rho\rho^{-2}\partial(\rho^2\bullet)/\partial\rho$ is a modified gradient operator.

2.1.4. Overall energy conservation

If the radiative intensity is known, then any other derived quantities such as radiative heat flux vector, incident radiation, radiation energy density, volumetric radiation source term (or divergence of radiative heat flux vector), absorbed radiative power per unit volume, etc., can be readily calculated. The radiative heat flux vector $\mathbf{q}_\lambda$ ($\mathrm{W/(m^2\mu m)}$) and incident radiation G ($\mathrm{W/(m^2\mu m)}$) are calculated based on radiative intensity as

$$\mathbf{q}_\lambda(\mathbf{r})=\int_{4\pi}I_\lambda(\mathbf{r},\mathbf{\Omega})\mathbf{\Omega}d\Omega,\qquad G_\lambda(\mathbf{r})=\int_{4\pi}I_\lambda(\mathbf{r},\mathbf{\Omega})d\Omega\tag{1.26}$$

The total radiative heat flux vector $\mathbf{q}$ and total incident radiation G can be calculated by a spectral integration with wavelength to $\mathbf{q}_\lambda$ and G_λ, respectively. The net spectral radiative heat flux onto a surface element $q_{s,\lambda}$ ($\mathrm{W/(m^2\mu m)}$) can thus be calculated from $q_{s,\lambda}=\mathbf{q}_\lambda\bullet\mathbf{n}_w$. The spectral radiation energy density u_λ ($\mathrm{J/(m^3\mu m)}$) is

$$u_\lambda(\mathbf{r})=\frac{n_\lambda}{c}\int_{4\pi}I_\lambda(\mathbf{r},\mathbf{\Omega})d\Omega=\frac{n_\lambda}{c}G_\lambda(\mathbf{r})\tag{1.27}$$

The absorbed spectral radiative power per unit volume w_λ ($\mathrm{W/(m^3\mu m)}$) can be calculated from

$$w_\lambda(\mathbf{r})=\kappa_a G_\lambda(\mathbf{r})\tag{1.28}$$

The balance equation of spectral radiative heat flux can be obtained by integrating the RTE in Cartesian coordinates (Eq. (1.12)) over entire solid angle , that is

$$\nabla\bullet\mathbf{q}_\lambda=4\pi\kappa_{a,\lambda}I_{b,\lambda}-\kappa_{a,\lambda}G_\lambda\tag{1.29}$$

The left hand side of Eq. (1.29), namely, $\nabla\bullet\mathbf{q}_\lambda$ stands for the out-flow radiation power per unit volume, which thus can be understood as a volumetric radiation source term. the first term and the second term of the right hand side are the emitted radiation power and the absorbed radiation power per unit volume, respectively. Balance equation of total radiative heat flux can be obtained as

$$\nabla \bullet \mathbf{q} = \int_0^\infty \kappa_{a,\lambda} \left(4\pi I_{b,\lambda} - G_\lambda\right) d\lambda \tag{1.30}$$

which can be simplified for gray medium ($\kappa_{a,\lambda} = \kappa_a$ and $n_\lambda = n$ are constant) as

$$\nabla \bullet \mathbf{q} = \kappa_a \left(4\pi I_b - G\right) = \kappa_a \left(4n^2 \sigma T^4 - G\right) \tag{1.31}$$

where $\sigma = 5.67 \times 10^{-8}$ (W/(m^{2}K^4)) is the Stefan-Boltzmann constant.

If temperature field is to be determined, and only radiation heat transfer is considered, the equation of overall energy conservation can be written as

$$\rho C \frac{\partial T}{\partial t} = Q'''_{rad} = \kappa_a \left(G - 4n^2 \sigma T^4\right) \tag{1.32}$$

where $Q'''_{rad} = -\nabla \bullet \mathbf{q}$ (W/m^3) denotes the equivalent radiative heat source, ρ (Kg/m^3) is the density, C (J/(Kg K)) is the specific heat capacity of the medium, At equilibrium, the temperature field can be determined as

$$T = \left(\frac{G}{4n^2 \sigma}\right)^{\frac{1}{4}} \tag{1.33}$$

If combined mode heat transfer of conduction and radiation is considered, the governing equation of overall energy conservation can be written as

$$\begin{aligned} \rho C \frac{\partial T}{\partial t} &= \nabla \bullet \left(k \nabla T\right) + Q'''_{rad} \\ &= \nabla \bullet \left(k \nabla T\right) + \kappa_a \left(G - 4n^2 \sigma T^4\right) \end{aligned} \tag{1.34}$$

where k (W/(m K)) is the heat conductivity of medium. If the convection heat transfer is further considered, the overall energy conservation equation can be written as

$$\begin{aligned} \rho C \left(\frac{\partial T}{\partial t} + \mathbf{u} \bullet \nabla T\right) &= \nabla \bullet \left(k \nabla T\right) + Q'''_{rad} + Q'''_f \\ &= \nabla \bullet \left(k \nabla T\right) + \kappa_a \left(G - 4n^2 \sigma T^4\right) + Q'''_f \end{aligned} \tag{1.35}$$

where $\mathbf{u}$ (m/s) is the fluid velocity vector, Q'''_f denotes the volumetric heat source other than thermal radiation, such as from viscous friction, chemical reaction, etc.

2.1.5. Boundary conditions for RTE

The inflow radiative intensity at the boundary walls must be set before the solution of the RTE. Generally speaking, three processes contribute to the emanated radiative intensity at the boundary walls, namely, the emission, reflection and transmission. For a diffuse emitting and reflecting opaque wall, the boundary condition can be written as

$$I_\lambda(\mathbf{r}_w,\mathbf{\Omega}) = \varepsilon_{w\lambda} I_{b,\lambda}[T(\mathbf{r}_w)] + \frac{1-\varepsilon_{w,\lambda}}{\pi}\int_{\mathbf{n}_w\bullet\mathbf{\Omega}'>0} I_\lambda(\mathbf{r}_w,\mathbf{\Omega}')\left|\mathbf{n}_w\bullet\mathbf{\Omega}'\right| d\Omega' ,\ \mathbf{n}_w\bullet\mathbf{\Omega}<0 \quad (1.36)$$

where $\varepsilon_{w\lambda}$ is the wall spectral emissivity, $\mathbf{n}_w$ is the normal vector of the wall pointing outside the enclosure. The boundary condition for diffuse wall (Eq. (1.36)) can also be written as (Modest 2013)

$$I_\lambda(\mathbf{r}_w,\mathbf{\Omega}) = I_{b,\lambda}[T(\mathbf{r}_w)] + \frac{1-\varepsilon_{w,\lambda}}{\pi\varepsilon_{w\lambda}}\mathbf{q}\bullet\mathbf{n}_w, \qquad \mathbf{n}_w\bullet\mathbf{\Omega}<0 \quad (1.37)$$

For real opaque rough surfaces, there will also be significant part of radiation reflection at the specular direction. As such, the wall reflection can be separated into a diffuse reflection part and a specular reflection part. In this case, the boundary condition can be written as

$$I_\lambda(\mathbf{r}_w,\mathbf{\Omega}) = \varepsilon_{w\lambda} I_{b,\lambda}[T(\mathbf{r}_w)] + \frac{\rho^d_{w,\lambda}}{\pi}\int_{\mathbf{n}_w\bullet\mathbf{\Omega}'>0} I_\lambda(\mathbf{r}_w,\mathbf{\Omega}')\left|\mathbf{n}_w\bullet\mathbf{\Omega}'\right| d\Omega' + \rho^s_{w,\lambda} I_\lambda(\mathbf{r}_w,\mathbf{\Omega}^s) \quad (1.38)$$

where $\rho^d_{w,\lambda}$ and $\rho^s_{w,\lambda}$ is the diffuse and specular reflectivity respectively, $\mathbf{\Omega}^s$ is the corresponding incident direction of specular reflection, which can be determined as $\mathbf{\Omega}^s = \mathbf{\Omega} - 2(\mathbf{\Omega}\bullet\mathbf{n}_w)\mathbf{n}_w$.

If an external radiative source, such as a laser, a lamp or solar beam is irradiated to a medium with semitransparent walls, the boundary condition can be written as

$$\begin{aligned} I_\lambda(\mathbf{r}_w,\mathbf{\Omega}) = {} & \varepsilon_{w\lambda} I_{b,\lambda}[T(\mathbf{r}_w)] + \frac{\rho^d_{w,\lambda}}{\pi}\int_{\mathbf{n}_w\bullet\mathbf{\Omega}'>0} I_\lambda(\mathbf{r}_w,\mathbf{\Omega}')\left|\mathbf{n}_w\bullet\mathbf{\Omega}'\right| d\Omega' + \rho^s_{w,\lambda} I_\lambda(\mathbf{r}_w,\mathbf{\Omega}^s) \\ & + \tau_{w\lambda} I_{ext}(\mathbf{r}_w,\mathbf{\Omega}) \end{aligned} \quad (1.39)$$

where $\tau_{w\lambda}$ is spectral transmittance of the semitransparent wall, $I_{ext}(\mathbf{r}_w,\mathbf{\Omega})$ is the radiative intensity of the external source.

2.1.6. Numerical properties of the classical RTE

The classical RTE (Eq. (1.12)) can be written shortly as

$$\mathbf{\Omega}\bullet\nabla I + \beta I = S \quad (1.40)$$

where S is the source term accounting for thermal emission and in-scattering contribution. The wavelength subscript is omitted for brevity. The first term of the left hand side of Eq. (1.40) can be seen as a convection term with a convection velocity of $\mathbf{\Omega}$, namely, μ, η and ξ are taken as the velocity in x-, y- and z- directions, respectively. Hence the RTE can be considered as a special kind of convection-diffusion equation without the diffusion term

(Chai et al. 2000b). The convection-dominated property is a source of numerical stability, which may cause unphysical numerical results and shows strong ray effects (Chai et al. 2000a).

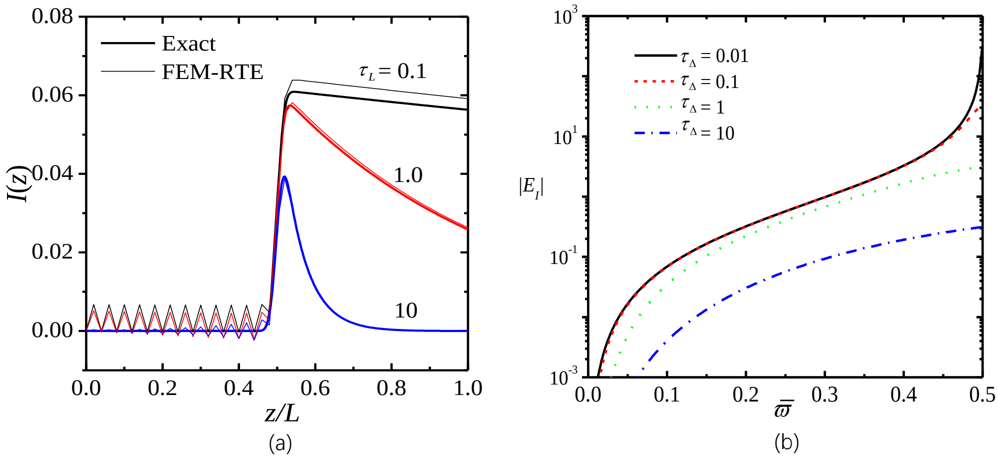

Fig. 5. Example results illustrating the numerical stability of the first order RTE. (a) Intensity distribution solved by finite element method for the Gaussian shaped emissive source problem, (b) theoretical frequency domain relative error of the RTE discretized using central difference scheme.

In order to illustrate the numerical stability of the first order RTE, Fig. 5 (a) shows the example results solved by a finite element method discretization of the first order RTE for a 1D case with a Gaussian shaped emissive source at different optical thickness excerpted from Ref. (Zhao and Liu 2007a). The solved radiative intensity distribution shows significant unphysical oscillations, which is a good demonstration of the instability issue caused by the convection-dominated characteristics of the RTE. Following the theoretical framework presented in Ref. (Zhao et al. 2013), the solution error can be predicted in frequency domain as shown in Fig. 5 (b). The frequency range of the reduced frequency $\bar{\varpi} = \Delta s \varpi / 2\pi$ is plotted in [0, 0.5], ϖ denotes the angular frequency in Fourier analysis, Δs is the grid spacing. This is based on the fact that the maximum frequency (or shortest wavelength) of a harmonic that can propagate on a uniform grid of spacing Δs is $\pi / \Delta s$ (or wavelength $2\Delta s$), namely, $\bar{\varpi}$ = 0.5. It can be seen that the relative error of intensity $|E_I|$ increases with $\bar{\varpi}$ for different grid optical thickness, and the maximum relative error occur at $\bar{\varpi}$ = 0.5 with a huge relative error greater than 300 for τ_Δ = 0.01. Hence significant error can be observed at around $\bar{\varpi}$ = 0.5, interpreting the observed high frequency unphysical oscillations in Fig. 5 (a). The solution errors (especially at the high frequency) obtained by the RTE reduces significantly with the increasing of grid optical thickness τ_Δ, indicating the solution error will decrease for problem with larger extinction coefficient on a specified grid, interpreting the observed decreasing of unphysical oscillations with increasing optical thickness in Fig. 5 (a).

2.2. The second order form of RTE

The classical form of the RTE under different coordinate systems has been presented in previous section. The convection-dominated characteristics of the RTE may cause unphysical oscillation in the numerical results as discussed in previous section. This type of instability occurs in many numerical methods, such as finite difference methods, finite element methods and meshless methods, etc., if no special stability treatment is taken (Chai et al. 2000b). It has been demonstrated that the classical RTE can be transformed into a new equation with a naturally introduced second order diffusion term to circumvent the stability issue. In this section, several second order form of RTEs are presented, including the even-parity formulation of RTE (EPRTE), the second order radiative transfer equation (SORTE) and its variants.

2.2.1. The even-parity formulation

The EPRTE is the first attempt that transforms the classic RTE into an equation with second order diffusion term, hence eliminates the convection-dominated property. The EPRTE was initially proposed in the field of neutron transport and has been used for decades. Song and Park (Song and Park 1992) initially applied the EPRTE in heat transfer field. It has been applied to DOM (Cheong and Song 1997) and FEM (Fiveland and Jessee 1995) discretization. In this approach, new variables, i.e., even- and odd-parity intensities are defined as function of radiative intensity both at forward direction and backward direction,

$$\psi_{\mathrm{E}}(\mathbf{r},\mathbf{\Omega})=\frac{1}{2}\left[I(\mathbf{r},\mathbf{\Omega})+I(\mathbf{r},-\mathbf{\Omega})\right] \tag{1.41}$$

$$\psi_{\mathrm{O}}(\mathbf{r},\mathbf{\Omega})=\frac{1}{2}\left[I(\mathbf{r},\mathbf{\Omega})-I(\mathbf{r},-\mathbf{\Omega})\right] \tag{1.42}$$

By adding and subtracting of the RTE (Eq. (1.12)) for forward direction $\mathbf{\Omega}$ and backward direction $-\mathbf{\Omega}$, yielding the governing equations of $\psi_{\mathrm{E}}(\mathbf{r},\mathbf{\Omega})$ and $\psi_{\mathrm{O}}(\mathbf{r},\mathbf{\Omega})$ for isotropic scattering media as,

$$\mathbf{\Omega}\bullet\nabla\psi_{\mathrm{O}}+\beta\psi_{\mathrm{E}}=\kappa_a I_b+\frac{\kappa_s}{2\pi}\int_{2\pi}\psi_{\mathrm{E}}(\mathbf{r},\mathbf{\Omega}')\mathrm{d}\Omega' \tag{1.43}$$

$$\mathbf{\Omega}\bullet\nabla\psi_{\mathrm{E}}+\beta\psi_{\mathrm{O}}=0 \tag{1.44}$$

These two equations can be decoupled. From Eq. (1.44), $\psi_{\mathrm{O}}=-\beta^{-1}\mathbf{\Omega}\bullet\nabla\psi_{\mathrm{E}}$, which is substituted into the first term of Eq. (1.43) to obtain a second order diffusion type of equation of ψ_{E}, namely, the EPRTE,

$$-\mathbf{\Omega}\bullet\nabla\left(\beta^{-1}\mathbf{\Omega}\bullet\nabla\psi_{\mathrm{E}}\right)+\beta\psi_{\mathrm{E}}=\kappa_a I_b+\frac{\kappa_s}{2\pi}\int_{2\pi}\psi_{\mathrm{E}}(\mathbf{r},\mathbf{\Omega}')\mathrm{d}\Omega' \tag{1.45}$$

It is noted that the angular integration for the scattering term is only over half solid angular space. Since this is a second order partial differential equation, boundary condition both at the inflow and outflow boundaries should be prescribed. Following similar approach, by adding and subtracting of the boundary condition (Eq.(1.36)) for forward direction $\mathbf{\Omega}$ and backward direction $-\mathbf{\Omega}$, the boundary conditions for ψ_{E} at inflow ($\mathbf{n}_w \bullet \mathbf{\Omega} < 0$) and out flow ($\mathbf{n}_w \bullet \mathbf{\Omega} > 0$) boundaries are obtained as

$$\begin{aligned} &\psi_{\mathrm{E}}(\mathbf{r}_w, \mathbf{\Omega}) - \beta^{-1}\mathbf{\Omega} \bullet \nabla \psi_{\mathrm{E}} \\ &= \varepsilon_w I_b(\mathbf{r}_w) + \frac{1-\varepsilon_w}{\pi} \int_{\mathbf{n}_w \bullet \mathbf{\Omega}' > 0} \left[\psi_{\mathrm{E}}(\mathbf{\Omega}, \mathbf{r}_w) + \beta^{-1}\mathbf{\Omega} \bullet \nabla \psi_{\mathrm{E}} \right] \left| \mathbf{n}_w \bullet \mathbf{\Omega}' \right| d\Omega' \end{aligned} \tag{1.46}$$

and

$$\begin{aligned} &\psi_{\mathrm{E}}(\mathbf{r}_w, \mathbf{\Omega}) + \beta^{-1}\mathbf{\Omega} \bullet \nabla \psi_{\mathrm{E}} \\ &= \varepsilon_w I_b(\mathbf{r}_w) + \frac{1-\varepsilon_w}{\pi} \int_{\mathbf{n}_w \bullet \mathbf{\Omega}' > 0} \left[\psi_{\mathrm{E}}(\mathbf{\Omega}, \mathbf{r}_w) - \beta^{-1}\mathbf{\Omega} \bullet \nabla \psi_{\mathrm{E}} \right] \left| \mathbf{n}_w \bullet \mathbf{\Omega}' \right| d\Omega' \end{aligned} \tag{1.47}$$

respectively.

2.2.2. The second order RTEs

The SORTE (Zhao and Liu 2007a) and its variant (Zhao et al. 2013) proposed recently, are diffusion-type equations similar to the heat conduction equation in anisotropic medium. Its governing variable is the radiative intensity, as compared to the EPRTE, of which the governing variable is the even-parity of radiative intensity. These two approaches share similar stability due to the same basic underlying principle. The using of radiative intensity as solution variable is more convenient and easier to be applied to complex radiative transfer problems for the SORTEs, such as anisotropic scattering.

The SORTE is rather easy to be derived based on the RTE. From Eq. (1.7), it is rearranged to have

$$I = -\beta^{-1}\frac{\mathrm{d}I}{\mathrm{d}s} + (1-\omega) I_b + \frac{\omega}{4\pi}\int_{4\pi} I(s, \mathbf{\Omega}')\Phi(\mathbf{\Omega}' \bullet \mathbf{\Omega}) d\Omega' \tag{1.48}$$

where $\omega = \kappa_s / \beta$ is the single scattering albedo. Substituting of this relation back into the first term of the RTE, the SORTE is then obtained,

$$-\frac{\mathrm{d}}{\mathrm{d}s}\left[\beta^{-1}\frac{\mathrm{d}I}{\mathrm{d}s}\right] + \beta I = \beta S - \frac{\mathrm{d}S}{\mathrm{d}s} \tag{1.49}$$

where S is the source function defined as

$$S = (1-\omega) I_b + \frac{\omega}{4\pi}\int_{4\pi} I(\mathbf{\Omega}', s)\Phi(\mathbf{\Omega}' \bullet \mathbf{\Omega}) d\Omega' \tag{5}$$

Following the approach in Section 1.1.2, the SORTE can be written in Cartesian coordinate as

$$-\mathbf{\Omega}\bullet\nabla\left[\beta^{-1}\mathbf{\Omega}\bullet\nabla I\right]+\beta I=\beta S-\mathbf{\Omega}\bullet\nabla S \tag{1.50}$$

and rewritten as

$$\nabla\bullet\left(\bar{\mathbf{K}}\bullet\nabla I\right)=\beta(I-S)+\mathbf{\Omega}\bullet\nabla S \tag{1.51}$$

where $\bar{\mathbf{K}}=\beta^{-1}\mathbf{\Omega\Omega}$, which is similar to the tensorial heat conductivity for anisotropic medium, and the terms at the right hand side can be viewed as effective heat source.

Similar to the EPRTE, the boundary condition for the SORTE should be prescribed both at the inflow and outflow boundaries. Since the governing variable is radiative intensity, the boundary condition is straight forward, which are given at the inflow and out flow boundary as (Zhao and Liu 2007a)

$$I(\mathbf{r}_w,\mathbf{\Omega})=\varepsilon_w I_b(\mathbf{r}_w)+\frac{1-\varepsilon_w}{\pi}\int_{\mathbf{n}_w\bullet\mathbf{\Omega}'>0} I(\mathbf{r}_w,\mathbf{\Omega}')\left|\mathbf{n}_w\bullet\mathbf{\Omega}'\right|d\Omega',\quad \mathbf{n}_w\bullet\mathbf{\Omega}<0 \tag{1.52}$$

$$\mathbf{\Omega}\bullet\nabla I(\mathbf{r}_w,\mathbf{\Omega})+\beta I(\mathbf{r}_w,\mathbf{\Omega})=\beta S(\mathbf{r}_w,\mathbf{\Omega}),\quad \mathbf{n}_w\bullet\mathbf{\Omega}>0 \tag{1.53}$$

Note that the inflow boundary condition for SORTE is the same for that of the RTE, and the outflow boundary condition is just the RTE itself.

Following the similar principle, the modified SORTE (MSORTE) was proposed (Zhao et al. 2013), in which no β^{-1} coefficient appears, hence it is better in dealing with inhomogeneous media where some locations have very small/zero extinction coefficient. The MOSRTE is obtained by applying the stream operator d/ds once to the RTE, which can be written in ray path coordinate as

$$\frac{\mathrm{d}^2 I}{\mathrm{d}s^2}+\frac{\mathrm{d}\beta I}{\mathrm{d}s}=\frac{\mathrm{d}\beta S}{\mathrm{d}s} \tag{1.54}$$

and in Cartesian coordinate system as

$$(\mathbf{\Omega}\bullet\nabla)^2 I+\mathbf{\Omega}\bullet\nabla(\beta I)=\mathbf{\Omega}\bullet\nabla(\beta S) \tag{1.55}$$

The boundary conditions for the MSORTE are the same as that for the SORTE.

2.2.3. Numerical properties of the second order RTE

The second order form of RTE contains a second order diffusion term, which circumvents the convection-dominated characteristics of the RTE, hence is numerically stable. The numerical properties of the RTE, SORTE, and MSORTE has been studied theoretically using Fourier analysis (Zhao et al. 2013), which confirms the stability of the second order forms of RTE. Fig. 6 gives a comparison of the predicted relative solution error in frequency domain for the first order and second order form of RTEs. As can be seen, at high frequency (ϖ closes to 0.5, which is the frequency of the unphysical oscillations), the relative error for the central difference discretization of the second order form of RTEs is far less than (two orders of magnitude) that of the RTE, proving the numerical stability of the second order form of RTEs.

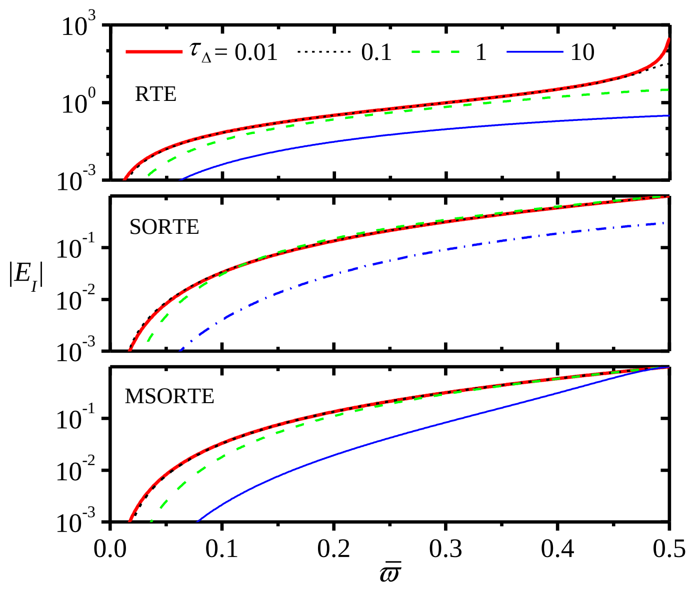

Fig. 6. The frequency domain distribution of solution error for the central difference discretization based on the RTE, the MSORTE and the SORTE at different grid optical thickness (Zhao et al. 2013).

2.3. The radiative transfer equation in refractive media

Due to the structural characteristics of a material or a possible temperature, pressure, and composition dependency, the refractive index of a media may be a function of spatial position. In this case, the ray goes along a curved path determined by the Fermat principle rather than along the straight lines. The formulation of the RTEs presented in previous section implicitly assumed straight line ray path. The effect of ray curvature or gradient index refraction has to be taken into account to formulate the radiative transfer equation in refractive media. Hence the RTE in uniform index media cannot be applied to gradient index media. The radiative heat transfer in semitransparent media with graded index is of significant importance in thermo-optical systems, atmospheric radiation, ocean optics, etc., and has evoked wide interest of many researchers (Zhu et al. 2011; Asllanaj and Fumeron 2010; Sun and Li 2009; Liu 2006; Xia et al. 2002; Ben Abdallah and Le Dez 2000b, a). In this section, the radiative transfer equation in gradient refractive index media and its formulation under different coordinate system are presented.

2.3.1. Ray path coordinate system formulation

When a light beam propagates in gradient index media, its direction will gradually change due to the effect of gradient of refractive index, besides the attenuation and augmentation effect caused by absorption, scattering and emission processes, as shown in Fig. 7. The governing equation of radiative transfer in gradient index media can be considered as an extension of the RTE to take into account the effect of gradient of refractive index.

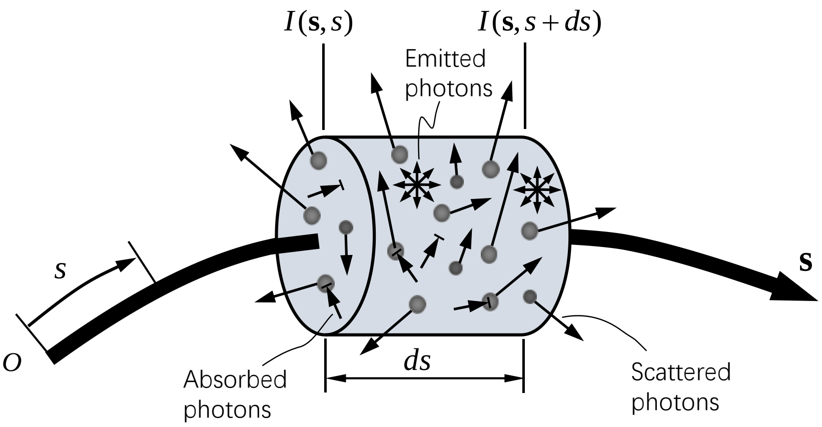

Fig. 7. Schematic of light transport in gradient index participating medium and variables definition in ray path coordinate.

The variation of radiative intensity along the curved ray path can be attributed to two mechanisms, the first is due to the variation of refractive index, and the second is from any other processes as discussed in participating media of uniform refractive index distribution. The total variation of radiative intensity along the curved ray path can be written as

$$\mathrm{d}I_\lambda(s,n(s),\mathbf{s}) = \frac{\partial I_\lambda(s,n(s),\mathbf{s})}{\partial s}ds + \frac{\partial I_\lambda(s,n(s),\mathbf{s})}{\partial n}dn \quad (1.56)$$

where the first term on the right hand side stands for the variation caused by the common processes of absorption, scattering and emission, which can be expressed based on the RTE in uniform refractive index media as

$$\frac{\partial I_\lambda(s,n(s),\mathbf{s})}{\partial s} = -\beta_\lambda I_\lambda(\mathbf{s},s) + \kappa_{a,\lambda} I_{b,\lambda}[T(s)] + \frac{\kappa_{s,\lambda}}{4\pi}\int_{4\pi} I_\lambda(s,\mathbf{\Omega}')\Phi_\lambda(\mathbf{\Omega}'\bullet\mathbf{s})\mathrm{d}\Omega' \quad (1.57)$$

The second term stands for the variation only caused by variation of refractive index, which is needed to be explicitly calculated. The Clausius invariant relation for transparent gradient index media gives $d\left[I_\lambda/n^2\right]=0$, from which the second term in Eq. (1.56) can be obtained as

$$\frac{\partial I_\lambda}{\partial n}dn = 2\frac{I_\lambda}{n}dn \quad (1.58)$$

Substituting Eq. (1.58) into Eq. (1.56), then the radiative transfer equation in gradient index medium (GRTE) in Lagrange form along the ray coordinate can be obtained as

$$n^2\frac{d}{ds}\left[\frac{I_\lambda(s,\mathbf{s})}{n^2}\right] + \beta_\lambda I_\lambda(\mathbf{s},s) = \kappa_{a,\lambda} I_{b,\lambda}[T(s)] + \frac{\kappa_{s,\lambda}}{4\pi}\int_{4\pi} I_\lambda(s,\mathbf{\Omega}')\Phi_\lambda(\mathbf{\Omega}'\bullet\mathbf{s})\mathrm{d}\Omega' \quad (1.59)$$

By expanding the Lagrangian stream operator in Eulerian frame (Eq. (1.8)), the transient GRTE is obtained,

$$\begin{aligned}&\frac{n_\lambda}{c}\frac{\partial I_\lambda(s,t,\mathbf{s})}{\partial t}+n^2\frac{\partial}{\partial s}\left[\frac{I_\lambda(s,t,\mathbf{s})}{n^2}\right]+\beta_\lambda I_\lambda(s,t,\mathbf{s})\\&=\kappa_{a,\lambda}I_{b,\lambda}[T(s)]+\frac{\kappa_{s,\lambda}}{4\pi}\int_{4\pi}I_\lambda(s,t,\mathbf{\Omega}')\Phi_\lambda(\mathbf{\Omega}'\bullet\mathbf{s})\mathrm{d}\Omega'\end{aligned} \tag{1.60}$$

Note that the GRTE doesn't contain information about the curved ray path. To solve the equation, the ray equation (Born and Wolf 1970) must be solved, that is

$$\frac{\mathrm{d}}{\mathrm{d}s}(n\mathbf{s})=\nabla n \tag{1.61}$$

The wavelength subscript will be omitted without loss of generality. More detailed derivation, including the polarization effect, refers to Zhao et al. 2012b.

2.3.2. Cartesian coordinate system formulation

To formulation the GRTE in Cartesian coordinate system, the stream operator needs to be explicitly expressed in this system. Assuming the radiative intensity is expressed as $I(\mathbf{r},\mathbf{\Omega})=I(x,y,z,\theta,\varphi)$, then the stream operator can be expanded as

$$\begin{aligned}\frac{d}{ds}&=\frac{dx}{ds}\frac{\partial}{\partial x}+\frac{dy}{ds}\frac{\partial}{\partial y}+\frac{dz}{ds}\frac{\partial}{\partial z}+\frac{d\theta}{ds}\frac{\partial}{\partial\theta}+\frac{d\varphi}{ds}\frac{\partial}{\partial\varphi}\\&=\mathbf{\Omega}\bullet\nabla+\frac{d\theta}{ds}\frac{\partial}{\partial\theta}+\frac{d\varphi}{ds}\frac{\partial}{\partial\varphi}\end{aligned} \tag{1.62}$$

To obtain the explicit formulation of the two angular derivatives, i.e., $d\theta/ds$ and $d\varphi/ds$ the ray equation (Eq. (1.61)) must be applied. Following the derivation in (Liu 2006), they can be written as

$$\frac{\mathrm{d}\varphi}{\mathrm{d}s}=\frac{1}{\sin\theta}\left(\mathbf{s}_1\bullet\frac{\nabla n}{n}\right),\quad\frac{\mathrm{d}\theta}{\mathrm{d}s}=\frac{1}{\sin\theta}\left[\left(\xi\mathbf{\Omega}-\mathbf{k}\right)\bullet\frac{\nabla n}{n}\right] \tag{1.63}$$

where $\mathbf{s}_1$ is an auxiliary vector defined as $\mathbf{s}_1=-\sin\varphi\mathbf{i}+\cos\varphi\mathbf{j}$. Substituting Eqs. (1.62), (1.63) into the GRTE in ray coordinate (Eq.(1.59)) and after some manipulations, the final conservative form of the GRTE in Cartesian coordinate system can be obtained as

$$\begin{aligned}&\mathbf{\Omega}\bullet\nabla I(\mathbf{r},\mathbf{\Omega})+\frac{1}{\sin\theta}\frac{\partial}{\partial\theta}\left[I(\mathbf{r},\mathbf{\Omega})\left(\xi\mathbf{\Omega}-\mathbf{k}\right)\right]\bullet\frac{\nabla n}{n}\\&+\frac{1}{\sin\theta}\frac{\partial}{\partial\varphi}\left[I(\mathbf{r},\mathbf{\Omega})\mathbf{s}_1\right]\bullet\frac{\nabla n}{n}+(\kappa_a+\kappa_s)I(\mathbf{r},\mathbf{\Omega})\\&=\kappa_a I_b(\mathbf{r})+\frac{\kappa_s}{4\pi}\int_{4\pi}I(\mathbf{r},\mathbf{\Omega}')\Phi(\mathbf{\Omega},\mathbf{\Omega}')\,d\Omega'\end{aligned}\tag{1.64}$$

The complete derivation refers to the work of Liu (Liu 2006). As compared to the RTE in Cartesian coordinate system (Eq. (1.12)), it is seen that there are two additional terms related to the gradient of refractive index (the second and third term) appears in Eq. (1.64), which are also terms about derivatives of angular variable θ and φ, and are usually called angular redistribution terms in literatures. It is angular redistribution terms that accounts for the effect of gradient refractive index distribution.

2.3.3. Formulation in other coordinate systems

The formulation of GRTE in cylindrical and spherical coordinate system are presented here. Two types of the cylindrical coordinate system are considered as shown in Fig. 3. Following similar procedure outlined in Section 1.3.2, the GRTE in the Type I cylindrical coordinate system (*ρ-Ψ-z-θ-φ*) can be derived and written in conservative form as (Liu et al. 2006)

$$\begin{aligned}&\mathbf{\Omega}\bullet\tilde{\nabla}_{\mathrm{I}}I-\frac{1}{\rho}\frac{\partial\eta I}{\partial\varphi}\\&+\frac{1}{\sin\theta}\left\{\frac{\partial}{\partial\theta}\left[\left((\xi\mathbf{\Omega}-\mathbf{e}_z)\bullet\frac{\nabla n}{n}\right)I\right]+\frac{\partial}{\partial\varphi}\left[\left(\mathbf{s}_1\bullet\frac{\nabla n}{n}\right)I\right]\right\}\\&+(\kappa_a+\kappa_s)I(\mathbf{r},\mathbf{\Omega})\\&=\kappa_a I_b(\mathbf{r})+\frac{\kappa_s}{4\pi}\int_{4\pi}I(\mathbf{r},\mathbf{\Omega}')\Phi(\mathbf{\Omega},\mathbf{\Omega}')\,d\Omega'\end{aligned}\tag{1.65}$$

where $\mathbf{\Omega}=\mu\mathbf{e}_\rho+\eta\mathbf{e}_\Psi+\xi\mathbf{e}_z$ is the local direction vector of the beam, $\mu=\sin\theta\cos\varphi$, $\eta=\sin\theta\sin\varphi$, $\xi=\cos\theta$, $\mathbf{e}_\rho$, $\mathbf{e}_\Psi$ and $\mathbf{e}_z$ are the unit coordinate vectors, $\tilde{\nabla}_{\mathrm{I}}(\bullet)=\mathbf{e}_\rho\rho^{-1}\partial(\rho\,\bullet)/\partial\rho+\mathbf{e}_\Psi\rho^{-1}\partial(\bullet)/\partial\Psi+\mathbf{e}_z\rho^{-1}\partial(\bullet)/\partial z$ is a modified gradient operator in the Type I cylindrical coordinate system, the auxiliary vector is defined as $\mathbf{s}_1=-\mathbf{e}_\rho\sin\varphi+\mathbf{e}_\Psi\cos\varphi$.

Similarly, the GRTE in the Type II cylindrical coordinate system (*Ψ-z-ρ-θ-φ*) can be obtained and written in conservative form as (Zhang et al. 2010; Zhao et al. 2012b)

$$\begin{aligned}
&\mathbf{\Omega}\bullet\tilde{\nabla}_{\mathrm{II}}I-\frac{1}{\rho\sin\theta}\frac{\partial}{\partial\theta}\left[\mu^{2}I\right]+\frac{1}{\rho}\frac{\partial}{\partial\varphi}\left[\xi\sin\varphi\cos\varphi I\right]\\
&+\frac{1}{\sin\theta}\left\{\frac{\partial}{\partial\theta}\left[\left((\xi\mathbf{\Omega}-\mathbf{e}_{z})\bullet\frac{\nabla n}{n}\right)I\right]+\frac{\partial}{\partial\varphi}\left[\left(\mathbf{s}_{1}\bullet\frac{\nabla n}{n}\right)I\right]\right\}\\
&+(\kappa_{a}+\kappa_{s})I(\mathbf{r},\mathbf{\Omega})\\
&=\kappa_{a}I_{b}(\mathbf{r})+\frac{\kappa_{s}}{4\pi}\int_{4\pi}I(\mathbf{r},\mathbf{\Omega}')\Phi(\mathbf{\Omega},\mathbf{\Omega}')\,d\Omega'
\end{aligned}\tag{1.66}$$

where $\mathbf{\Omega}=\mu\mathbf{e}_{\Psi}+\eta\mathbf{e}_{z}+\xi\mathbf{e}_{\rho}$ is the local direction vector of the beam, the auxiliary vector $\mathbf{s}_{1}=-\sin\varphi\mathbf{e}_{\Psi}+\cos\varphi\mathbf{e}_{z}$, $\tilde{\nabla}_{\mathrm{II}}(\bullet)=\mathbf{e}_{\Psi}\rho^{-1}\partial(\bullet)/\partial\Psi+\mathbf{e}_{z}\partial(\bullet)/\partial z+\mathbf{e}_{\rho}\rho^{-1}\partial(\rho\bullet)/\partial\rho$ is a modified gradient operator in the Type II cylindrical coordinate system.

The definition of the spherical coordinate system (Θ-Ψ-ρ-θ-φ) is shown in Fig. 4. Following the procedure outlined in Section 1.3.2, the GRTE in the spherical coordinate system can be obtained and written in conservative form as follows (Liu et al. 2006).

$$\begin{aligned}
&\mathbf{\Omega}\bullet\tilde{\nabla}I-\frac{1}{\rho\sin\theta}\frac{\partial\sin^{2}\theta I}{\partial\theta}-\frac{\cot\Theta}{\rho}\frac{\partial\eta I}{\partial\varphi}\\
&+\frac{1}{\sin\theta}\left\{\frac{\partial}{\partial\theta}\left\{\left[(\xi\mathbf{\Omega}-\mathbf{e}_{\rho})\bullet\frac{\nabla n}{n}\right]I\right\}+\frac{\partial}{\partial\varphi}\left[\left(\mathbf{s}_{1}\bullet\frac{\nabla n}{n}\right)I\right]\right\}\\
&+(\kappa_{a}+\kappa_{s})I(\mathbf{r},\mathbf{\Omega})\\
&=\kappa_{a}I_{b}(\mathbf{r})+\frac{\kappa_{s}}{4\pi}\int_{4\pi}I(\mathbf{r},\mathbf{\Omega}')\Phi(\mathbf{\Omega},\mathbf{\Omega}')\,d\Omega'
\end{aligned}\tag{1.67}$$

where $\mathbf{\Omega}=\mu\mathbf{e}_{\Theta}+\eta\mathbf{e}_{\Psi}+\xi\mathbf{e}_{\rho}$ is the local direction vector of the beam, $\mathbf{s}_{1}=-\sin\varphi\mathbf{e}_{\Theta}+\cos\varphi\mathbf{e}_{\Psi}$ is an auxiliary vector, the gradient operator $\tilde{\nabla}$ is defined as $\tilde{\nabla}(\bullet)=\mathbf{e}_{\Theta}(\rho\sin\Theta)^{-1}\partial(\sin\Theta\bullet)/\partial\Theta+\mathbf{e}_{\Psi}(\rho\sin\Theta)^{-1}\partial/\partial\Psi+\mathbf{e}_{\rho}\rho^{-2}\partial(\rho^{2}\bullet)/\partial\rho$.

3. Solution techniques of the radiative transfer equation

In this section, four fundamental deterministic methods for radiative transfer in participating media are introduced, including the spherical harmonics method, the DOM, FVM and FEM. The spherical harmonics method is highly efficient for complex multidimensional problems. The DOM, FVM and FEM are versatile, with good accuracy and convenient to be coupled with conduction and convection solvers. Note that several important aspects of numerical solution of radiative tranfser equation are not covered in this chapter, such as the spectral models for non-gray media, problems with collimated irradiation and transient radiative transfer.

3.1. Spherical harmonics method

Spherical harmonics method also known as P_N approximation, is one basic type of method to solve radiative transfer. Especially, the lower order approximations, such as the P_1 and P_3 approximation, have achieved broad range of applications (Mengüç and Viskanta 1985; Mengüç and Iyer 1988). It is considered to suffer less from the ray effects, which can significantly deteriorate the accuracy of discrete ordinates method. In the spherical harmonics method, the angular dependence of radiative intensity is expanded as a series of spherical harmonics, and the expansion coefficients are finally formulated into a set of partial differential equations to be solved. In this approach, the radiative intensity is approximated as

$$I(\mathbf{r},\mathbf{\Omega}) = \sum_{l=0}^{\infty} I_l^m(\mathbf{r}) Y_l^m(\mathbf{\Omega}) \tag{1.68}$$

where $Y_l^m(\mathbf{\Omega})$ are spherical harmonics, which are orthogonal functions in solid angular space, $I_l^m(\mathbf{r})$ are the corresponding expansion coefficient. The governing equations for $I_l^m(\mathbf{r})$ can be obtained by substituting Eq. (1.68) into the RTE (Eq. (1.12)) and then weighted angular integration is performed with different orders of spherical harmonics.

It is usually very cumbersome to obtain the equations of $I_l^m(\mathbf{r})$, especially for higher order approximation for multidimensional problems. Here, the P_1 approximation is presented. For the P_1 approximation, the expansion in Eq. (1.68) is truncated for $l > 1$. Four terms are retained in the series and the radiative intensity can be shortly written as

$$I(\mathbf{r},\mathbf{\Omega}) = a(\mathbf{r}) + \mathbf{b}(\mathbf{r}) \bullet \mathbf{\Omega} \tag{1.69}$$

Substituting of Eq. (1.69) into the RTE (Eq. (1.12)) to obtain

$$\begin{aligned} &\mathbf{\Omega}\bullet\nabla a(\mathbf{r}) + (\mathbf{\Omega}\mathbf{\Omega}) : \nabla\mathbf{b}(\mathbf{r}) + \beta\left[a(\mathbf{r}) + \mathbf{b}(\mathbf{r})\bullet\mathbf{\Omega}\right] \\ &= \kappa_a I_b + \kappa_s a(\mathbf{r}) + \kappa_s g \mathbf{b}(\mathbf{r})\bullet\mathbf{\Omega} \end{aligned} \tag{1.70}$$

Note that the last term is obtained using the following relation

$$\int_{4\pi} \mathbf{\Omega}'\Phi(\mathbf{\Omega}'\bullet\mathbf{\Omega})\,\mathrm{d}\Omega' = \int_{4\pi} \begin{bmatrix} \sin\theta\cos\varphi \\ \sin\theta\sin\varphi \\ \cos\theta \end{bmatrix} \Phi(\cos\theta)\sin\theta d\theta d\varphi = 4\pi g \mathbf{\Omega} \tag{1.71}$$

where g is by definition the asymmetry factor of the scattering phase function. Equation (1.71) is general, not limited to the linear anisotropic scattering phase function. The following two equations are obtained by integrating Eq. (1.70) for the zeroth and first order moment.

$$\nabla\bullet\mathbf{b}(\mathbf{r}) = 3\kappa_a\left[I_b - a(\mathbf{r})\right] \tag{1.72}$$

$$\mathbf{b}(\mathbf{r}) = -\frac{1}{\beta - \kappa_s g}\nabla a(\mathbf{r}) \tag{1.73}$$

The P_1 approximation equation can be obtained by substituting Eq. (1.73) into Eq.(1.72). The physical meaning of $a(\mathbf{r})$ and $\mathbf{b}(\mathbf{r})$ can be made clear by substituting Eq. (1.69) into the definition formula of radiative heat flux and incident radiation (Eq. (1.26)), which yields $a(\mathbf{r}) = \frac{G(\mathbf{r})}{4\pi}$, and $\mathbf{b}(\mathbf{r}) = \frac{3}{4\pi}\mathbf{q}$. Finally, the P_1 approximation equations are summarized below.

G equation:
$$-\nabla \bullet \left[\frac{1}{3(\beta - \kappa_s g)} \nabla G \right] = \kappa_a (4\pi I_b - G) \tag{1.74}$$

q equation:
$$\mathbf{q} = -\frac{1}{3(\beta - \kappa_s g)} \nabla G \tag{1.75}$$

I equation:
$$I(\mathbf{r}, \mathbf{\Omega}) = \frac{1}{4\pi}\left[G(\mathbf{r}) + 3\mathbf{q}(\mathbf{r}) \bullet \mathbf{\Omega} \right] \tag{1.76}$$

By using the I equation, the boundary condition for diffuse emission and reflection boundary can be determined as

$$\frac{2-\varepsilon}{\varepsilon} \frac{2}{3(\beta - \kappa_s g)} \mathbf{n}_w \bullet \nabla G + G = 4\pi I_{bw} \tag{1.77}$$

At radiative equilibrium, namely, $\nabla \bullet \mathbf{q} = 0$, and $G = 4\pi I_b$, the q-equation (Eq.(1.75)) indicates

$$\mathbf{q} = -\frac{4\pi}{3(\beta - \kappa_s g)} \nabla I_b \tag{1.78}$$

This is the same as the Rosseland approximation (or diffusion approximation).

As can be seen, only one equation is needed to be solved (G equation) for radiative heat transfer, hence it is highly efficient to be used to analyze engineering radiative transfer problems. Even though, the P_1 can give reasonable results for optically thick media. However, it may produce significant errors for optically thin media, in case the approximation Eq. (1.69) fails. The accuracy of P_1 approximation can be improved by using higher order spherical harmonics, such as P_3 approximation. There are also a variant of P_N approximation, called the simplified P_N-approximation (SP_N) (Larsen et al. 2002), which can generate equations consistent with P_1 approximation at low order and can be relatively easy to be extended to higher order.

3.2. Discrete ordinates method

The discrete ordinates method for the solution of radiative transfer was first proposed by Chandrasekhar (Chandrasekhar 1960). It was then introduced to solve neutron transport, such as the work of Carlson and Lathrop (Carlson and Lathrop 1965). Fiveland (Fiveland 1984) and Truelove (Truelove 1988) applied the method to solve general radiative heat transfer problems. A recent review of the DOM and FVM was given by Coelho (Coelho 2014). In the following, the basic principle of the method is presented. The solution of radiative transfer equation requires discretization of both angular and spatial domains. The idea of DOM is to represent the angular space by a discretized set of directions, and only radiative intensity at these discrete directions is solved. Each direction is associated with a quadrature weight. Both the directions and the weight are chosen carefully to ensure accuracy of angular integration, which is important for discretizing the in-scattering term and calculating the radiative heat flux. After the angular discretization is finished, the original integral-differential form of RTE becomes a set of coupled partial differential equations, which can then be discretized and solved by traditional techniques for solving partial differential equations.

3.2.1. Angular discretization

The angular space is discretized as a set of discrete directions, $\mathbf{\Omega}_m = \mu_m \mathbf{i} + \eta_m \mathbf{j} + \xi_m \mathbf{k}$, then the RTE (Eq. (1.12)) can be written into a set of partial differential equations, namely, the discrete ordinates equations,

$$\mathbf{\Omega}_m \bullet \nabla I_m(\mathbf{r}) + \beta I_m(\mathbf{r}) = \kappa_a I_b(\mathbf{r}) + \frac{\kappa_s}{4\pi}\sum_{m'=1}^{M} I_{m'}(\mathbf{r})\Phi(\mathbf{\Omega}_{m'} \bullet \mathbf{\Omega}_m)\, w_{m'},\ m = 1,\ldots,M \quad (1.79)$$

where w_m is the weight of direction $\mathbf{\Omega}_m$ for angular quadrature, M is the total number of discrete discretions. For the opaque and diffuse boundary, the boundary condition for each discrete ordinate equation is written as

$$I_w(\mathbf{\Omega}_m) = \varepsilon_w I_{bw} + \frac{1-\varepsilon_w}{\pi}\sum_{\mathbf{n}_w \bullet \mathbf{\Omega}_{m'} > 0} I_w(\mathbf{\Omega}_{m'})\left|\mathbf{n}_w \bullet \mathbf{\Omega}_{m'}\right| w_{m'},\ \ \mathbf{\Omega}_m \bullet \mathbf{n}_w < 0 \quad (1.80)$$

By definition, the radiative heat flux and incident radiation are determined as

$$\mathbf{q}(\mathbf{r}) = \sum_{m=1}^{M} I^m(\mathbf{r})\mathbf{\Omega}^m\, w^m, \qquad G(\mathbf{r}) = \sum_{m=1}^{M} I^m(\mathbf{r})\, w^m \quad (1.81)$$

The definition of the angular discretization includes the selection of the set discrete directions (ordinates) and the design of the related angular quadrature, which is critical about the accuracy of the method. There are several criteria proposed on the selection of angular discretization and the weights (Fiveland 1984; Carlson and Lathrop 1965): (1) the symmetry criterion, namely, the discrete set of directions and weights should be the same after the rotation of $\pi/2$ about each principle axis (x-,y- and z-); (2) the full space moment preserving criterion, i.e., the angular quadrature defined based on the selected directions should satisfy the zeroth, first and second moments integrated over 4π, namely,

$$\int_{4\pi} d\Omega = 4\pi = \sum_{m=1}^{M} w^m \quad (1.82)$$

$$\int_{4\pi} \mathbf{\Omega} d\Omega = \mathbf{0} = \sum_{m=1}^{M} \mathbf{\Omega}^m w^m \tag{1.83}$$

$$\int_{4\pi} \mathbf{\Omega}\mathbf{\Omega} d\Omega = \frac{4\pi}{3}\boldsymbol{\delta} = \sum_{m=1}^{M} \mathbf{\Omega}^m \mathbf{\Omega}^m w^m \tag{1.84}$$

where $\mathbf{0}$ denotes the zero vector, $\boldsymbol{\delta}$ is the unit tensor; (3) the half space moment preserving criterion, i.e., the defined angular quadrature should preserve the first moment integration over 2π, requiring

$$\begin{aligned} \int_{\mu>0} \mu d\Omega &= \pi = \sum_{\mu_m>0} \mu_m w_m \\ \int_{\eta>0} \eta d\Omega &= \pi = \sum_{\eta_m>0} \eta_m w_m \\ \int_{\xi>0} \xi d\Omega &= \pi = \sum_{\xi_m>0} \xi_m w_m \end{aligned} \tag{1.85}$$

The most well known family of the discrete ordinates set is the S_N sets, initially proposed for simulation of neutron transport (Carlson and Lathrop 1965), which are also tabulated in the classic text books (Howell et al. 2011; Modest 2013). The angular discretization using the S_N discrete ordinates set is usually called S_N approximation. For the S_N approximation, such as S_2, S_4, or S_6, where N means the number of discrete direction cosines used for each principal direction. Total number of directions for the S_N-approximation is $M = N(N+2)$. Several other discrete ordinate sets were also proposed, such as the T_N sets by Thurgood et al. (Thurgood et al. 1995). A recent review of the angular discretization schemes in DOM was given by Koch and Becker (Koch and Becker 2004).

3.2.2. Spatial discretization

After angular discretization, the resulting discrete ordinates equations (Eq. (1.79)) for each direction $\mathbf{\Omega}^m$ can then be discretized by common methods for solving partial differential equations, such as finite difference method and FVM. Note that upwinding scheme is required to obtain reliable results considering the numerical property of the RTE discussed in Section 1.1.6, an alternative is to use the second order form of RTE for discretization.

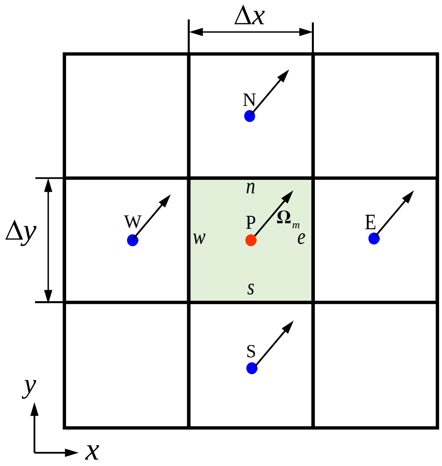

Fig. 8. Grid used to define the spatial discretization by using FVM.

Here, common FVM approach is used to discretize the discrete ordinates equation of DOM (Eq. (1.79)) to obtain the final algebraic equation. The advantage of FVM is that it is easy to be applied to unstructured mesh to solve problems with complex geometry. Fig. 8 shows the 2D grid used to define the FVM discretization scheme. The unknown radiative intensities are stored at the center of each grid cell. By integrating Eq. (1.79) over the control volume P and using the Gaussian divergence theorem to the first term to obtain

$$\Delta y\left(\mu_m I_{m,e}-\mu_m I_{m,w}\right)+\Delta x\left(\eta_m I_{m,n}-\eta_m I_{m,s}\right)+\beta_P I_{m,P}\Delta x\Delta y=S_{m,P}\Delta x\Delta y \tag{1.86}$$

where the subscript of capitalized letters denotes the value at cell center (*P*), and the subscript of small letters (e, w, n and s) denote values at the center of faces as shown in Fig. 8, $S_{m,P}$ is the source term defined as

$$S_{m,P}=S_m(\mathbf{r}_P)=\kappa_a I_b(\mathbf{r}_P)+\frac{\kappa_s}{4\pi}\sum_{m'=1}^{M}I_{m'}(\mathbf{r}_P)\,\Phi(\mathbf{\Omega}_{m'}\bullet\mathbf{\Omega}_m)\,w_{m'} \tag{1.87}$$

Since radiative intensities are stored at cell center only, interpolation of radiative intensity at faces to that at cell center is required to obtain the final algebraic equations. Using interpolation and supposing uniform grid, the face values can be interpolated using neighboring cell values as

$$I_{m,n}=\alpha_y I_{m,P}+(1-\alpha_y)I_{m,N}\,,\quad I_{m,e}=\alpha_x I_{m,P}+(1-\alpha_x)I_{m,E} \tag{1.88a}$$

$$I_{m,s}=\alpha_y I_{m,S}+(1-\alpha_y)I_{m,P}\,,\quad I_{m,w}=\alpha_x I_{m,W}+(1-\alpha_x)I_{m,P} \tag{1.88b}$$

where α_x and α_y are the interpolation parameters for x and y directions, respectively. Substituting Eq. (1.88) into Eq.(1.86), the final discretization can be written as

$$a_P I_{m,P} = a_N I_{m,N} + a_S I_{m,S} + a_W I_{m,W} + a_E I_{m,E} + b \tag{1.89}$$

where the discrete coefficients are determined as

$$\begin{aligned} &a_N = \eta_m \Delta x(\alpha_y - 1),\ a_E = \mu_m \Delta y(\alpha_x - 1),\ a_S = \eta_m \Delta x \alpha_y,\ a_W = \mu_m \Delta y \alpha_x \\ &a_P = a_N + a_S + a_W + a_E + \beta_P \Delta x \Delta y,\ \ b = S_{m,P} \Delta x \Delta y \end{aligned} \tag{1.90}$$

Different differencing schemes can be obtained by defining different interpolation parameters, such as, (1) step scheme (or first order upwind scheme), $\alpha_x = \max\left[\mu_m / |\mu_m|, 0\right]$ and $\alpha_y = \max\left[\eta_m / |\eta_m|, 0\right]$; (2) diamond scheme (or central difference scheme), $\alpha_x = \alpha_y = 1/2$. Coelho (Coelho 2002a) investigated higher order differencing schemes in DOM.

The resulting linear systems Eq. (1.89) can be solved element by element until convergence, or solved by sparse solvers. Since the source term contains radiative intensity of other directions, a global iteration is required to successively update the source terms for problems with scattering media and reflecting boundary conditions. The discretization presented above can be easily extended to 3D problems. The extension to unstructured mesh is presented in the next section.

3.3. Finite volume method

Raithby and Chui (Chui and Raithby 1992; Raithby and Chui 1990) firstly formulated FVM for solving radiative heat transfer problems. Chai and coworkers (Chai and Lee 1994; Chai et al. 1993) developed different variant implementations of FVM. A comprehensive review of the development of DOM and FVM was given recently by Coelho (Coelho 2014). In the FVM method, both the angular domain and the spatial domain are discretized by using control volume integration. The angular discretization in FVM is thus different from the DOM. The angular domain discretization in FVM uses structured mesh as shown in Fig. 9, while the spatial domain can be structured or unstructured. Though different from DOM, the FVM can be formulated in a very similar fashion with DOM. As such the major difference between DOM and FVM lies in the angular discretization.

3.3.1. Angular discretization

Integrating the RTE (Eq. (1.12)) over a small control angle of Ω^{ml} centered at direction $\mathbf{\Omega}^{ml}$ (the superscript *m* and *l* denotes the index of θ and φ discretization, respectively), and assuming the radiative intensity is constant over Ω^{ml}, it leads to

$$\int_{\Omega^{ml}} \mathbf{\Omega} d\Omega \bullet \nabla I^{ml}(\mathbf{r}) + \beta\, \Omega^{ml} I^{ml}(\mathbf{r}) = \Omega^{ml} S^{ml}(\mathbf{r}) \tag{1.91}$$

where $S^{ml}(\mathbf{r})$ is given as

$$S^{ml}(\mathbf{r}) = \kappa_a I_b(\mathbf{r}) + \frac{\kappa_s}{4\pi} \sum_{l'=1}^{N_\varphi} \sum_{m'=1}^{N_\theta} I^{m'l'}(\mathbf{r}) \bar{\Phi}(\mathbf{\Omega}^{m'l'} \bullet \mathbf{\Omega}^{ml}) \Omega^{m'l'} \tag{1.92}$$

In which $\bar{\Phi}(\mathbf{\Omega}^{m'l'} \bullet \mathbf{\Omega}^{ml}) = \dfrac{1}{\Omega^{m'l'} \Omega^{ml}} \int_{\Omega^{ml}} \int_{\Omega^{m'l'}} \Phi(\mathbf{\Omega}^{m'l'} \bullet \mathbf{\Omega}^{ml}) d\Omega' \, d\Omega$.

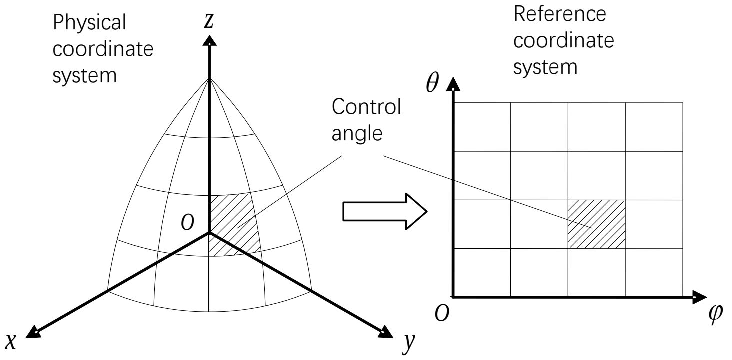

Fig. 9. Schematic of angular grid used in FVM discretization.

Dividing Ω^{ml} to both sides of Eq.(1.91), an equation in the form of discrete ordinates equation (Eq. (1.79)) is obtained, which is written as

$$\bar{\mathbf{\Omega}}^{ml} \bullet \nabla I^{ml}(\mathbf{r}) + \beta\, I^{ml}(\mathbf{r}) = S^{ml}(\mathbf{r}) \tag{1.93}$$

where $\bar{\mathbf{\Omega}}^{ml}$ is an averaged direction vector defined as

$$\bar{\mathbf{\Omega}}^{ml} = \frac{1}{\Omega^{ml}} \int_{\Omega^{ml}} \mathbf{\Omega} d\Omega \tag{1.94}$$

Note that $\bar{\mathbf{\Omega}}^{ml}$ can be calculated analytically (Murthy and Mathur 1998). Taking $\bar{\mathbf{\Omega}}^{ml}$ as the equivalent discrete direction in DOM, the quantities, such as heat flux, incident radiation, etc., can be calculated the same way as in the DOM.

3.3.2. Spatial discretization

Since mathematical form of Eq. (1.93) is the same as the discrete ordinates equation, the spatial FVM discretization procedure described in previous section for DOM can be directly applied. Here only formulation on unstructured mesh is introduced, which can also be applied to the DOM for spatial discretization. Considering the unknowns are stored in the center of the control volume cell, integrating Eq. (1.93) over a spatial control volume and applying the Gaussian divergence theorem to the first term leads to

$$\sum_{i=1}^{N_f} A_{f_i} I_{f_i}^{ml} \bar{\mathbf{\Omega}}^{ml} \bullet \mathbf{n}_{f_i} + \beta_P I_P^{ml} \Delta V_P = S_P^{ml} \Delta V_P \tag{1.95}$$

where the subscript f_i denotes value at the i-th face of control volume centered at *P*, the subscript P denotes value at point P, $\mathbf{n}$ is the surface normal, A is area of the face, and ΔV_P is the volume of the control volume centered at *P*. To complete the discretization, the intensity defined at surface should be interpolated to nodal values (volume center), which can be generally written as

$$I_{f_i}^{ml} = \alpha_i I_P^{ml} + (1-\alpha_i) I_{P_i}^{ml} \tag{1.96a}$$

where P_i denotes the center of the neighboring cell of *i*-th face of the cell *P*. With this closure relation, the final FVM discretization can be written as

$$a_P I_P^{ml} = \sum_{i=1}^{N_f} a_{P_i} I_{P_i}^{ml} + b^{ml} \tag{1.97}$$

where the discrete coefficients are given as

$$\begin{aligned} a_P &= \sum_{i=1}^{N_f} A_{f_i} \alpha_i \bar{\mathbf{\Omega}}^{ml} \bullet \mathbf{n}_{f_i} + \beta_P \Delta V_P \\ a_{P_i} &= A_{f_i} (\alpha_i - 1) \bar{\mathbf{\Omega}}^{ml} \bullet \mathbf{n}_{f_i} \\ b^{ml} &= S_P^{ml} \Delta V_P \end{aligned} \tag{1.98}$$

If the step scheme (or first order upwind) is used, then $\alpha_i = \max\left[\bar{\mathbf{\Omega}}^{ml} \bullet \mathbf{n}_{f_i} \Big/ \left| \bar{\mathbf{\Omega}}^{ml} \bullet \mathbf{n}_{f_i} \right|, 0 \right]$. Equation (1.97) for each control angle can be solved element by element and iterated until convergence.

3.4. Finite element method

Fiveland and Jesse (Fiveland and Jessee 1994) were the first to apply the FEM to solve radiative heat transfer problems based on the differential form of RTE. Until recently, many variant implementations of FEM have been proposed (Liu 2004b; W. An et al. 2005; Zhao and Liu 2007a; Zhang et al. 2016). After angular discretization, as described in Section 3.2 and 3.3, the RTE becomes a set of partial differential equations, i.e., the discrete ordinates equations, which can then be solved by common numerical method for solving partial differential equations. Similar to FVM, FEM is another versatile method that can be applied to solve a broad range of partial differential equations appeared in scientific and engineering problems, hence is very appealing for multiphysics simulation. The feature of FEM is that it usually owns higher order of accuracy as compared to the FVM. In the FEM, the unknown radiative intensity is first approximated as a series of shape functions, which is then combined with the weighted residual approach to discretize the RTE, finally a sparse linear system is obtained and solved by general solvers. Here the FEM for solving the RTE is introduced.

3.4.1. Function approximation

The solid angular space discretization is by the common discrete ordinates approach, such as the S_N sets or the FVM approach described in section 3.2 and 3.3. The radiative intensity for each discrete direction $\mathbf{\Omega}_m$ can be approximated using the FEM shape functions ϕ_i at each solution nodes, namely

$$\tilde{I}_m(\mathbf{x}) \simeq \sum_{i=1}^{N_{sol}} I_{m,i}\phi_i(\mathbf{x}) \tag{1.99}$$

where $I_{m,i}$ are the expansion coefficients, which are also the values of the radiative intensity of direction $\mathbf{\Omega}_m$ at node *i* (namely, $I_{m,i} = I\left(\mathbf{\Omega}_m, \mathbf{x}_i\right)$) due to the Kronecker delta property of the FEM shape functions. For example, the global shape function at node *i* for the 1D linear element can be written as

$$\phi_i\,(x) = \begin{cases} \left(x - x_{i-1}\right)/\Delta x, & x_{i-1} \le x < x_i \\ \left(x_{i+1} - x\right)/\Delta x, & x_i \le x < x_{i+1} \\ 0, & \text{otherwise} \end{cases} \tag{1.100}$$

which is also graphically shown in Fig. 10 (a) for better understanding.

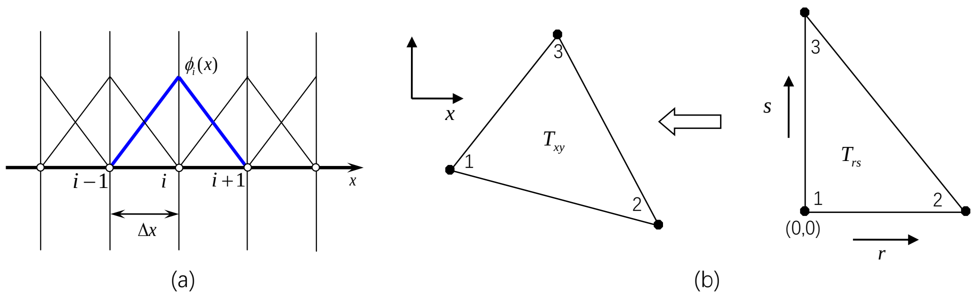

Fig. 10. (a) Schematic of nodal shape function of 1D linear elements in FEM. (b) transform of linear elements defined on reference space to physical space

Generally, for multidimensional complex elements, the shape function on an element can be first defined in a reference space, and then transformed to the physical space, as shown in Fig. 10 (b), where a linear triangular element is taken as example. For 2D triangular element, the three shape functions defined in reference space (*r*-*t*) can be written as

$$\Gamma_1(r,s) = 1 - r - s,\ \Gamma_2(r,s) = r,\ \Gamma_3(r,s) = s \tag{1.101}$$

which can be transformed to obtain the shape function in physical space (*x*-*y*) as

$$\phi_i(x(r,s),y(r,s)) = \Gamma_i(r,s)\,, \qquad i=1,2,3 \tag{1.102}$$

The coordinate system transformation from reference element $T_{rs}:\{(0,0),(1,0),(0,1)\}$ to physical element $T_{xy}:\{(\hat{x}_1,\hat{y}_1),(\hat{x}_2,\hat{y}_2),(\hat{x}_3,\hat{y}_3)\}$ is defined as

$$x=\sum_{i=1}^{3}\hat{x}_i\,\Gamma_i(r,s), \quad y=\sum_{i=1}^{3}\hat{y}_i\,\Gamma_i(r,s) \tag{1.103}$$

where $\hat{x}_i,\hat{y}_i$, $i=1,2,3$ denote the coordinates of the nodes that define the triangular element.

3.4.2. Weighted residual approach

The discrete ordinates equation (Eq. (1.79)) can be written as

$$\mathbf{\Omega}_m \bullet \nabla I_m(\mathbf{r}) + \beta\, I_m(\mathbf{r}) = S_m(\mathbf{r}) \tag{1.104}$$

where the source term $S_m(\mathbf{r},\mathbf{\Omega})$ are defined as

$$S_m(\mathbf{r}) = \kappa_a I_b(\mathbf{r}) + \frac{\kappa_s}{4\pi}\sum_{m'=1}^{M} I_{m'}(\mathbf{r})\,\Phi(\mathbf{\Omega}_{m'} \bullet \mathbf{\Omega}_m)\, w_{m'} \tag{1.105}$$

Using weighted residual approach, Eq. (1.104) is weighted by a set of weight functions $W_j(\mathbf{r})$ and integrated over the solution domain, which leads to (Liu et al. 2008)

$$\left\langle \mathbf{\Omega}_m \bullet \nabla I_m(\mathbf{r}), W_j(\mathbf{r})\right\rangle + \left\langle \beta\, I_m(\mathbf{r}), W_j(\mathbf{r})\right\rangle = \left\langle S_m(\mathbf{r}), W_j(\mathbf{r})\right\rangle \tag{1.106}$$

where the inner product $<\bullet,\bullet>$ is defined as $<f,g>=\int_V fg\mathrm{d}V$.

By substituting the approximated radiative intensity (Eq.(1.99)) into weighted residual approach equation (Eq.(1.106)) and choosing different set of weight functions, a discrete set of linear equations can be obtained, which can be written in matrix form as

$$\mathbf{K}_m \mathbf{u}_m = \mathbf{h}_m \tag{1.107}$$

where $\mathbf{u}_m = \left[u_{m,i}\right]_{i=1,N_{sol}} = \left[I_m(\mathbf{r}_i)\right]_{i=1,N_{sol}}$, $\mathbf{K}_m$ and $\mathbf{h}_m$ are conventionally called stiff matrix and load vector, respectively, which are different for different FEM discretization. The selection of the weighted function results in different FEM discretization schemes, such as for Galerkin scheme (Galerkin FEM), which choose $W_j = \phi_j$, and least-squares scheme (LSFEM) to choose $W_j = \mathbf{\Omega}_m \bullet \nabla\phi_j + \beta\phi_j$. Note that the LSFEM formulation can also be derived based on functional minimization procedure.

For the Galerkin FEM discretization, $\mathbf{K}_m$ and $\mathbf{h}_m$ are obtained as (Liu et al. 2008)

$$\mathbf{K}_m = \left[K_{m,ji}\right]_{j=1,N_{sol};i=1,N_{sol}} = <\mathbf{\Omega}_m \bullet \nabla\phi_i, \phi_j> + <\beta\phi_i, \phi_j> \tag{1.108a}$$

$$\mathbf{h}_m = \left[h_{m,j}\right]_{j=1,N_{sol}} =< S_m, \phi_j > \tag{1.108b}$$

For the LSFEM discretization, $\mathbf{K}_m$ and $\mathbf{h}_m$ are obtained as (Zhao et al. 2012a)

$$\begin{aligned}\mathbf{K}_m &= \left[K_{m,ji}\right]_{j=1,N_{sol};i=1,N_{sol}} \\ &=< \mathbf{\Omega}_m \bullet \nabla\phi_i, \mathbf{\Omega}_m \bullet \nabla\phi_j > + < \beta\phi_i, \beta\phi_j > \\ &+ < \beta\phi_i, \mathbf{\Omega}_m \bullet \nabla\phi_j > + < \mathbf{\Omega}_m \bullet \nabla\phi_i, \beta\phi_j >\end{aligned} \tag{1.109a}$$

$$\mathbf{h}_m = \left[h_{m,j}\right]_{j=1,N_{sol}} =< S_m, \beta\phi_j > + < S_m, \mathbf{\Omega}_m \bullet \nabla\phi_j > \tag{1.109b}$$

It is noted that the stiff matrix produced by LSFEM is symmetric and positively definite, which is a very good numerical property.

The accuracy in the imposing of this type of boundary condition is very important for the overall solution accuracy. One accurate method for imposing the Dirichlet type boundary condition is operator collocation approach. In this approach, the row of stiff matrix $\mathbf{K}_m$ corresponding to the inflow boundary nodes is replaced with the discrete operator of the related boundary condition. Similar modifications are also applied to the load vector $\mathbf{h}_m$. The modification algorithm are formulated as below (the modifications are only conducted for nodes on the inflow boundary, namely, $\mathbf{n}_w(\mathbf{r}_j) \bullet \mathbf{\Omega}_m < 0$).

$$K_{m,ji} = \delta_{ji}, \tag{1.110a}$$

$$h_{m,j} = I_0(\mathbf{r}_j, \mathbf{\Omega}_m). \tag{1.110b}$$

where $I_0(\mathbf{r}_j, \mathbf{\Omega}_m)$ stands for the radiative intensity at the boundary given by Eq. (1.80).

The FEM has also been successfully applied to the second order form of RTEs to avoid the stability problem caused by the convection-dominated property of the first order RTE and this kind of FEM has been demonstrated to be numerically stable and accurate (Fiveland and Jessee 1994; Zhao and Liu 2007a; Zhang et al. 2016).

3.5. Solution methods for RTE in refractive media

Many numerical methods have been developed for the solution of radiative transfer in gradient index media, which include the curved ray-tracing based methods (Ben Abdallah and Le Dez 2000b; Ben Abdallah et al. 2001; Huang et al. 2002a, b; Liu 2004a; Wang et al. 2011), and the methods based on discretization of the GRTE. The ray tracing is usually cumbersome and time consuming in calculation. Lemonier and Le Dez (Lemonnier and Le Dez 2002) pioneered the discrete ordinates method for solving the GRTE. Their work is for one-dimensional problem. Thereafter, Liu (Liu 2006) formulated the discrete ordinates equation of GRTE for general multidimensional problems, which forms the basis for the solution of radiative transfer in gradient index media. It plays similar role as the discrete ordinates equation of RTE in uniform index media. Based on the discrete ordinates equation, the spatial discretization techniques, such as FVM and FEM can be readily applied for solution. Besides the FEM and FVM, many other numerical methods have been developed to solve radiative heat transfer in gradient index media based on the discrete ordinates equation of GRTE (Zhao and Liu 2007b; Sun and Li 2009; Asllanaj and Fumeron 2010; Zhang et al. 2015).

In this section, only the solution techniques based on the discretization of the GRTE are introduced. Generally, the basic principle to solve the GRTE is the same as that for radiative transfer in uniform index media. As outlined in previous sections, the first is to discretize the angular space to transform the integral-differential equation into a set of partial differential equations, namely, the discrete ordinates equations. The second step is to spatially discretize the discrete ordinates equations, which can be done by common methods such as finite difference, FVM and FEM, etc. However, the GRTE differs from the RTE for containing two angular redistribution terms, which have derivatives with respect to angular variables. The discrete ordinates equation of GRTE is the key for different solution methods. However, to determine the discrete ordinates equations for GRTE is not so straight forward as that for the RTE (Lemonnier and Le Dez 2002; Liu 2006).

In the following, the discrete ordinates equation for GRTE is presented. The detailed derivation refers to (Liu 2006; Liu and Tan 2006). Formally, the discrete ordinates equations of GRTE can be written as

$$\begin{aligned}&\mathbf{\Omega}^{m,n}\cdot\nabla I(\mathbf{r},\Omega^{m,n})+\left[\frac{1}{\sin\theta}\frac{\partial}{\partial\theta}\left\{I(\mathbf{r},\Omega)\left(\xi\mathbf{\Omega}-\mathbf{k}\right)\right\}\right]_{\Omega=\Omega^{m,n}}\bullet\frac{\nabla n}{n}\\&+\left[\frac{1}{\sin\theta}\frac{\partial}{\partial\varphi}\left(I(\mathbf{r},\Omega)\mathbf{s}_1\right)\right]_{\Omega=\Omega^{m,n}}\bullet\frac{\nabla n}{n}+(\kappa_a+\kappa_s)I(\mathbf{r},\Omega^{m,n})\\&=\kappa_a I_b+\frac{\kappa_s}{4\pi}\sum_{m'=1}^{N_\theta}\sum_{n'=1}^{N_\varphi}I(\mathbf{r},\Omega^{m',n'})\Phi(\Omega^{m',n'},\Omega^{m,n})w_\theta^{m'}w_\varphi^{n'}\end{aligned}\tag{1.111}$$

where piecewise constant angular quadrature (PCA) is used to discrete the angular space, in which the total solid angle is divided uniformly in the polar θ and azimuthal φ directions, defined as

$$\theta^m=(m-1/2)\Delta\theta\,,\ \ m=1,\cdots,N_\theta \tag{1.112a}$$

$$\varphi^n=(n-1/2)\Delta\varphi\,,\ \ n=1,\cdots,N_\varphi \tag{1.112b}$$

where $\Delta\theta = \pi / N_\theta$ and $\Delta\varphi = 2\pi / N_\varphi$ are steps for the discretization of polar and azimuthal angles, respectively, N_θ and N_φ are the corresponding number of divisions. For each discrete direction (m,n), the corresponding weight is

$$w_\theta^m = \cos\theta^{m-1/2} - \cos\theta^{m+1/2}, \qquad w_\varphi^n = \varphi^{n+1/2} - \varphi^{n-1/2}, \tag{1.113}$$

where $\theta^{m+1/2} = \left(\theta^m + \theta^{m+1}\right)/2$, $\varphi^{n+1/2} = \left(\varphi^n + \varphi^{n+1}\right)/2$.

The two angular redistribution terms can be formally discretized as

$$\left[\frac{1}{\sin\theta}\frac{\partial}{\partial\theta}\{I(\xi\mathbf{\Omega}-\mathbf{k})\}\bullet\frac{\nabla n}{n}\right]_{\Omega=\Omega^{m,n}} \simeq \frac{\chi_\theta^{m+1/2,n} I^{m+1/2,n} - \chi_\theta^{m-1/2,n} I^{m-1/2,n}}{w_\theta^m}, \tag{1.114a}$$

$$\left[\frac{1}{\sin\theta}\frac{\partial}{\partial\varphi}\left(I(\mathbf{r},\Omega)\mathbf{s}_1\right)\bullet\frac{\nabla n}{n}\right]_{\Omega=\Omega^{m,n}} \simeq \frac{\chi_\varphi^{m,n+1/2} I^{m,n+1/2} - \chi_\varphi^{m,n-1/2} I^{m,n-1/2}}{w_\varphi^n}. \tag{1.114b}$$

Details on determining the discrete coefficients of χ_θ and χ_φ were presented in Ref. (Liu 2006). Substituting of Eq. (1.114) into Eq. (1.64) and applying necessary closure relations (Liu 2006), the final discrete ordinates equation of GRTE can be obtained and expressed in a form similar to the discrete ordinates equation of RTE, i.e.,

$$\mathbf{\Omega}^{m,n}\bullet\nabla I^{m,n} + \tilde{\beta}^{m,n}(\mathbf{r}) I^{m,n} = \tilde{S}^{m,n}(\mathbf{r}), \tag{1.115a}$$

where the modified extinction coefficient $\tilde{\beta}^{m,n}(\mathbf{r})$ and modified source term $\tilde{S}^{m,n}(\mathbf{r})$ are

$$\begin{aligned}\tilde{\beta}^{m,n}(\mathbf{r}) &= \frac{1}{w_\theta^m}\max\left(\chi_\theta^{m+1/2,n},0\right) + \frac{1}{w_\theta^m}\max\left(-\chi_\theta^{m-1/2,n},0\right) \\ &\quad + \frac{1}{w_\varphi^n}\max\left(\chi_\varphi^{m,n+1/2},0\right) + \frac{1}{w_\varphi^n}\max\left(-\chi_\varphi^{m,n-1/2},0\right) + \left(\kappa_a + \kappa_s\right)\end{aligned} \tag{1.115a}$$

$$\begin{aligned}\tilde{S}^{m,n}(\mathbf{r}) &= n^2\kappa_a I_b + \frac{\kappa_s}{4\pi}\sum_{m'=1}^{N_\theta}\sum_{n'=1}^{N_\varphi} I^{m',n'}\Phi^{m',n';m,n} w_\theta^{m'} w_\varphi^{n'} \\ &\quad + \frac{1}{w_\theta^m}\max\left(-\chi_\theta^{m+1/2,n},0\right) I^{m+1,n} + \frac{1}{w_\theta^m}\max\left(\chi_\theta^{m-1/2,n},0\right) I^{m-1,n} \\ &\quad + \frac{1}{w_\varphi^n}\max\left(-\chi_\varphi^{m,n+1/2},0\right) I^{m,n+1} + \frac{1}{w_\varphi^n}\max\left(\chi_\varphi^{m,n-1/2},0\right) I^{m,n-1}\end{aligned} \tag{1.115b}$$

The recursion formulas for $\chi_\theta^{m+1/2,n}$ and $\chi_\varphi^{m,n+1/2}$ are giving below.

$$\chi_\theta^{m+1/2,n} - \chi_\theta^{m-1/2,n} = \frac{w_\theta^m}{\sin\theta^m}\left[\frac{\partial(\xi\mathbf{\Omega})}{\partial\theta}\bullet\frac{\nabla n}{n}\right]_{\Omega=\Omega^{m,n}} \tag{1.116a}$$

$$\chi_{\theta}^{1/2,n} = \chi_{\theta}^{N_\theta+1/2,n} = 0 \quad (1.116b)$$

$$\chi_{\varphi}^{m,n+1/2} - \chi_{\varphi}^{m,n-1/2} = \frac{w_{\varphi}^{n}}{\sin\theta^{m}}\left[\frac{\partial \mathbf{s}_1}{\partial\varphi}\bullet\frac{\nabla n}{n}\right]_{\Omega=\Omega^{m,n}} \quad (1.116c)$$

$$\chi_{\varphi}^{m,1/2} = \chi_{\varphi}^{m,N_\varphi+1/2} = \frac{1}{\sin\theta^{m}}\left(\mathbf{j}\bullet\frac{\nabla n}{n}\right) \quad (1.116d)$$

Similar to the discrete ordinates equations of RTE, Eq. (1.115) with boundary conditions are solved for each discrete direction. Since both $\tilde{\beta}^{m,n}(\mathbf{r})$ and $\tilde{S}^{m,n}(\mathbf{r})$ contain part of angular redistribution terms, which is different from the discrete-ordinates equation of RTE. The source term updating is always needed during the solution process. The spatial discretization techniques, such as FVM and FEM presented in previous sections can be readily applied to Eq. (1.115) for solution. Note that the discretization of the GRTE can also be conducted without relying on the discrete ordinates equation. Recently, Zhang et al. (Zhang et al. 2012) developed a hybrid FEM/FVM technique to solve the GRTE, in which the angular domain is discretized using FEM and the spatial domain is discretized using FVM, and the radiative intensities at all the directions are solved simultaneously at each spatial node. The idea of this approach follows the work of Coelho (Coelho 2005) for solving the RTE.

4. Numerical errors and accuracy improvement strategies

All numerical methods suffer from numerical errors. The MC method suffers from statistic errors, while the DOM, FVM and FEM suffer from space and angular discretization errors. Due to the significant importance in real applications, numerical errors for solving RTE has attracted the interest of many researchers (Chai et al. 1993; Ramankutty and Crosbie 1997; Coelho 2002b; Hunter and Guo 2015; Huang et al. 2011; Tagne Kamdem 2015). In this section, DOM is taken as an example method, and the numerical errors that appear in DOM and the related improvement strategies are discussed.

4.1. Origin of numerical errors in DOM

The ‘false scattering’ and ‘ray effects’ are terms to describe the characteristics of the numerical errors observed in numerical results of DOM. Literally, ‘false scattering’ means the effect of the numerical error behaving like scattering process, which was usually considered to be equivalent to numerical diffusion (Chai et al. 1993). The ‘ray effects’ stands for the unphysical bump that appears in the numerical results, which is attributed to the using of discrete number of directions to approximate the continuous angular variation of radiative intensity (Chai et al. 1993).

In order to understand the origin of the error phenomenon, it is necessary to analyze the source of errors in DOM. By carefully checking the DOM discretization of RTE and the calculation of heat flux and incident radiation, three major sources of errors can be identified, (1) error from the differencing scheme, which is related to the discretization of the differential operator in spatial domain; (2) error from the discretization of scattering term, which is related to the discretization of an integral operator in angular domain; (3) error from the calculation of heat flux or incident radiation, which is related to the discretization of another integral operator. Note that the third source is distinctly different from the second source, since it will appear even if the medium is non-scattering. What are the effect of these three source of errors? What is the relation of these three sources of errors with 'false scattering' and 'ray effects'? These will be discussed in the following sections.

4.2. Error from differencing scheme

A differencing scheme is required to discretize the differential operator in the discrete ordinates equation of RTE (Eq. (1.79)). Taking step scheme for example, which is equivalent to the first order upwind finite difference scheme. Assuming $\mu_m > 0$, it can be discretized for the x-direction as

$$\mu_m \frac{\partial I_m}{\partial x} \simeq \mu_m \frac{I_m(x) - I_m(x - \Delta x)}{\Delta x} \tag{1.117}$$

Using Taylor expansion, the right hand side of the above discretization can be written as

$$\mu_m \frac{I_m(x) - I_m(x - \Delta x)}{\Delta x} = \mu_m \frac{\partial I_m}{\partial x} + \left[\frac{1}{2}\mu_m \Delta x\right] \frac{\partial^2 I_m}{\partial x^2} + O(\Delta x^2) \tag{1.118}$$

As seen, an additional diffusion term appears (the second order term), which has a diffusion coefficient of $\mu_m \Delta x / 2$. Namely, the dominant error for step scheme is a diffusion process. This numerical diffusion will smooth the radiative intensity distribution, making additional radiative heat flux transport from high intensity region to low intensity region, similar to the heat conduction process. It is significantly different from the scattering process, such as, it only smears radiative flux of one direction, while the scattering process usually transfers energy from one direction to another direction. As such, this error is preferable to be called numerical diffusion. Hunter and Guo (Hunter and Guo 2015) derived the expression of numerical diffusion of several differencing schemes, including the step scheme, diamond scheme, and QUICK scheme. The numerical diffusion can be significantly reduced if a high order scheme is applied. For a low order scheme like the step scheme, the numerical diffusion will decrease with mesh refinement.

Fig. 11 (a) shows the solved heat flux by DOM with step scheme at coarse grid (15x15) and fine grid (125x125), in which the data are extracted from the work by Coelho (Coelho

2002b). The angular discretization is extremely fine, hence the effect of angular discretization error can be neglected, and only the effect of numerical diffusion is observed. At coarse grid, big numerical diffusion appears, and the heat flux value is always greater than the exact value, which agrees with the analysis presented above.

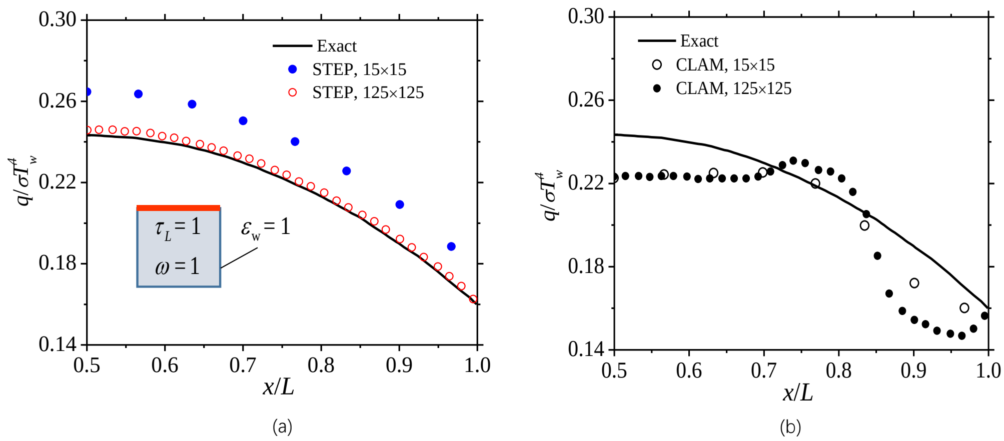

Fig. 11. Incident heat flux along the bottom wall to illustrate numerical diffusion and ray effects. (a) Step scheme, $N_\theta = N_\varphi$ =100 per octant, (b) CLAM scheme, S_8 approximation is used. Data are exacted from Ref. (Coelho 2002b). Insets shows the shape of enclosure, the top wall is hot and others are cold.

4.3. Scattering term discretization error

The DOM approximates the in-scattering term as

$$\int_{4\pi} I(\mathbf{\Omega}',\mathbf{r})\Phi(\mathbf{\Omega}'\bullet\mathbf{\Omega})\mathrm{d}\Omega' \simeq \sum_{m'=1}^{M} I_{m'}(\mathbf{r}_P)\Phi^{m'm} w_{m'} \tag{1.119}$$

This approximation will inevitably introduce discretization errors. Since the scattering phase function and radiative intensity distribution are usually complicated, this angular quadrature may introduce significant errors for scattering media, e.g., the phase function with strong forward peak. The discretization error of this term is considered to alter the contribution of original scattering phase function. By this understanding, this error induces unphysical scattering, i.e., false scattering, which changes the coupling of radiative intensity among different directions unphysically.

To improve the discretization accuracy of scattering phase function, several techniques have been proposed. The first is to modify the discrete phase function to ensure the exact energy conservation constraint, i.e.,

$$\sum_{m'=1}^{M} \Phi^{m'm} w_{m'} = 4\pi \tag{1.120}$$

The most common approach is to modify the phase function as follows (Liu et al. 2002)

$$\tilde{\Phi}^{m'm} = \Phi^{m'm}\left(\frac{1}{4\pi}\sum_{m'=1}^{M}\Phi^{m'm}\,w_{m'}\right)^{-1} \tag{1.121}$$

which will ensure $\tilde{\Phi}^{m'm}$ exactly satisfy the energy conservation relation.

Hunter and Guo (Hunter and Guo 2012a; Hunter and Guo 2012b) showed that the normalization given in Eq. (1.121) is not enough for strongly forward scattering phase function, e. g., asymmetry factor greater than 0.9. In this case, another constraint on conservation of asymmetry factor *g*, should also be satisfied for the modified scattering phase function to get reliable results, namely,

$$\sum_{m'=1}^{M}\Phi^{m'm}\,w_{m'}\cos(\Theta^{m'm}) = 4\pi g \tag{1.122}$$

They then devised new schemes to normalize the discrete scattering phase function to ensure both the conservation of energy (Eq. (1.120)) and the conservation of asymmetry factor be satisfied (Hunter and Guo 2012a, 2014). Detailed normalization procedure refers to the pioneer work of Hunter and Guo (Hunter and Guo 2012a). A recent work on comparison of the different normalization schemes for strongly forward scattering phase function was given by Granate et al. (Granate et al. 2016). The errors that arise from discretizatoin of the scattering term was also called ‘angular false scattering’ in Ref. (Hunter and Guo 2015).

4.4. Error from heat flux calculation

The phenomenon of ray effects is that the heat flux distribution contains unphysical bump pattern of errors, as shown in Fig. 11 (b). It mainly influences the solution accuracy of DOM when there are sharp gradients or discontinuities in the boundary conditions, temperature distribution, or radiative properties of the medium. Ray effects have been demonstrated to mainly rely on angular discretization (Lathrop 1968; Chai et al. 1993). Fig. 11 (b) shows the heat flux distribution along the bottom wall solved by CLAM scheme at a course (15x15) and fine (125x125) spatial grid, S_8 approximation is used for angular quadrature. It is known that CLAM scheme is a second-order accurate and bounded non-oscillatory scheme. However, even for the fine grid that spatial discretization is considered to be sufficiently accurate, there are still strong unphysical bump patterns in the heat flux distribution. Hence the numerial error featured with the bump pattern is unrelated with the spatial discretization. Furthermore, this kind of bump patterns contained in heat flux distribution still exists for the media without scattering (Coelho 2002b). Hence it cannot be attributed to the error from the scattering term. It has a distinct origin. Here the bump pattern of numerical error is attributed to the inaccurate heat flux calculation.

Fig. 12 (a) shows a typical configuration that has strong ray effects. In this case, only a confined load is located at the bottom and the heat flux distribution along the top wall is to be calculated. Considering the media is non-scattering, the incident radiative intensity at the top wall can be traced back to the load. Point O denotes the center of the top wall and A is a point located with a distance from the center. The blue and red lines start from O and A indicates the discrete ordinates directions, which are traced back to determine the intensities exactly. As can be seen, for point A, there are two directions intercepted with the load. As for the center point O, only one direction intercepts with the load.

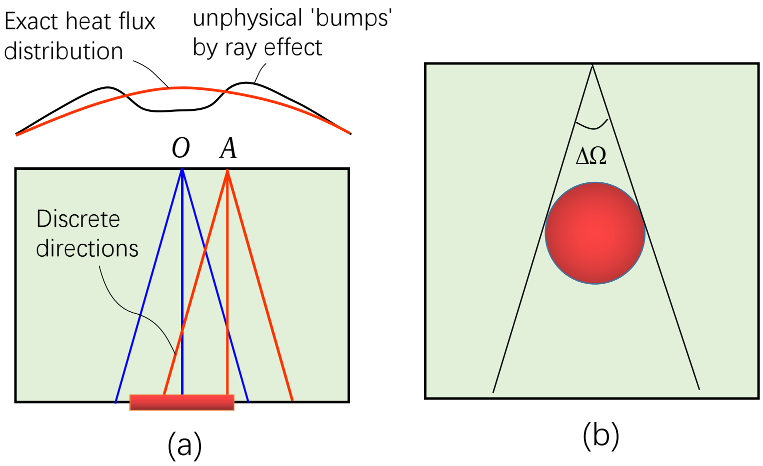

Fig. 12. Schematics to illustrate ray effects. (a) boundary confined load, (b) inside (volumetric) confined load.

If angular quadrature is used to calculate the heat flux, it is obvious that heat flux at point A will be greater than that at the center point O. This analysis agrees with former observations, such as the numerical results shown in Fig. 11 (b). Besides the confined boundary load, confined volumetric load (as shown in Fig. 12 (b)) will also induce ray effects as studied by Coelho (Coelho 2002b; Coelho 2004). The confinement of radiative intensity in a small solid angle is difficult to be accurately integrated, because only few discrete ordinates directions will be located in the small solid angle to do integration. The ray effects can be mitigated by refining the angular discretization (Chai et al. 1993; Li et al. 2003), however, this approach requires considerable computational effort. It can also be effectively mitigated by the modified discrete ordinates approach (Ramankutty and Crosbie 1997; Coelho 2002b; Coelho 2004), which treats the contributions from boundary load, and volumetric load to heat flux separately by solving a different transfer equation. Recently, several new approaches were proposed to mitigate the ray effects in FVM and DOM. More effective way to mitigate the ray effects in DOM is still an important subject of research (Huang et al. 2011; Tagne Kamdem 2015).

5. Conclusions

In this chapter, the classical radiative transfer equation and several variant forms of radiative transfer equation, the different solution techniques for the radiative transfer equations, and the numerical errors on the solution of radiative transfer equation and the related improvement strategies are presented and discussed. The classical RTE implies that light propagate through straight line. To analyze radiative transfer in gradient index media where light propagate through curved lines, the GRTE should be applied. Under Cartesian coordinate the GRTE contains two terms of angular derivatives as compared to the RTE, which account for the effect of gradient refractive index. The classical RTE is in a form of a first-order integral partial differential equation. It can be considered as a special kind of convection-diffusion equation with convection dominated property. This is also true for the GRTE. The convection-dominated property will induce numerical instability for numerical solution. The classical RTE can be transformed to second order forms and to avoid the stability problem.

Numerical methods to solve radiative transfer can be classified into two groups, (1) methods based on stochastic simulation and (2) the deterministic methods, which are usually formulated based on the integral or differential form of RTE. The MCM is a typical method of the first group, it is versatile and reliable, but usually time consuming since a huge number of photons need to be traced, and is inconvenient to be coupled with conduction and convection solvers, the latter are usually implemented using deterministic methods such as FVM and FEM. DOM is the typical method of the second group. The FVM can be considered as a special kind of DOM that the discrete ordinates equations are obtained based on the FVM. FEM is usually more accurate than the FVM, furthermore, it is very versatile and promising for the simulation of multiphysics processes including radiative heat transfer.

Three major sources of errors for numerical solution of RTE can be identified, (1) error from differencing scheme, which is related to the discretization of a differential operator; (2) error from the discretization of scattering term, which is related to the discretization of an angular integral operator; (3) error from the calculation of heat flux or incident radiation, which is related to the discretization of another angular integral operator. The first will induce numerical diffusion, in which radiative energy diffuses to the same direction. The second will induce unphysically altered phase function, hence is the true 'false scattering'. The third will induce unphysical bump pattern of errors in the flux distribution, also known as 'ray effects', which is attributed to inaccuracy of angular quadrature. But this is distinctly different from the second source, since it will appear even if the medium is non-scattering. Besides the errors mentioned above, it should be noted that the actual solution accuracy of radiative transfer problems also relies closely on the accuracy of measured material properties, such as absorption coefficient, scattering coefficient and scattering phase function, which should be cared for the solution of real problems.

Acknowledgements

The authors thank the supports by National Nature Science Foundation of China (Nos. 51336002, 51421063). The supports by the Fundamental Research Funds for the Central Universities (Grant No. HIT. NSRIF. 2013094, HIT.BRETIII.201415) are also greatly acknowledged.

Cross-References

- Introduction: Thermal Radiation Heat Transfer
- Radiative Transfer in Combustion Systems
- Monte Carlo Methods for Radiative Transfer
- Radiative Properties of Particles

- Radiative Properties of Gases
- Radiative Plasma Heat Transfer

References

Agrafiotis CC, Mavroidis I, Konstandopoulos AG, Hoffschmidt B, Stobbe P, Romero M, Fernandez-Quero V (2007) Evaluation of porous silicon carbide monolithic honeycombs as volumetric receivers/collectors of concentrated solar radiation. Sol Energy Mater Sol Cells 91 (6):474-488.

Asllanaj F, Fumeron S (2010) Modified finite volume method applied to radiative transfer in 2D complex geometries and graded index media. J Quant Spectrosc Radiat Transfer 111 (2):274-279

Ben Abdallah P, Charette A, Le Dez V (2001) Influence of a spatial variation of the thermo-optical constants on the radiative transfer inside an absorbing–emitting semi-transparent sphere. J Quant Spectrosc Radiat Transfer 70 (3):341-365

Ben Abdallah P, Le Dez V (2000a) Thermal emission of a semi-transparent slab with variable spatial refractive index. J Quant Spectrosc Radiat Transfer 67 (3):185-198

Ben Abdallah P, Le Dez V (2000b) Thermal field inside an absorbing-emitting semitransparent slab at radiative equilibrium with variable spatial refractive index. J Quant Spectrosc Radiat Transfer 65 (4):595-608

Benoit H, Spreafico L, Gauthier D, Flamant G (2016) Review of heat transfer fluids in tube-receivers used in concentrating solar thermal systems: Properties and heat transfer coefficients. Renewable and Sustainable Energy Reviews 55:298-315

Berberoglu H, Yin J, Pilon L (2007) Light transfer in bubble sparged photobioreactors for H2 production and CO2 mitigation. J Quant Spectrosc Radiat Transfer 32 (13):2273-2285

Born M, Wolf E (1970) Principles of Optics. 7th edn. Cambridge University Press, Cambridge

Carlson BG, Lathrop KD (1965) Transport theory: the method of discrete ordinates. In: Greenspan H, Kelber CN, Okrent D (eds) Computational Methods in Reactor Physics. Gordon and Breach, New York, pp 171–270

Chai JL, Cheng Q, Song JL, Wang ZC, Zhou HC (2015) The DRESOR method for one-dimensional transient radiative transfer in graded index medium coupled with BRDF surface. Int J Therm Sci 91:96-104.

Chai JC, Lee HO, Patankar SV (1993) Ray effect and false scattering in the discrete ordinates method. Numer Heat Transfer B 24 (4):373-389

Chai JC, Lee HS (1994) Finite-Volume Method for Radiation Heat Transfer. J Thermophys Heat Transfer 8 (32):419-425

Chai JC, Lee HS, Patankar SV (2000a) Finite-volume Method for Radiation Heat Transfer. Adv Numer Heat Transfer 2:109-141

Chai JC, Lee HS, Patankar SV (2000b) Finite-volume Method for Radiation Heat Transfer. In: Minkowycz WJ, Sparrow EM (eds) Advances in numerical heat transfer, vol 2. Taylor & Francis, New York, pp 109-141

Chandrasekhar S (1960) Radiative Transfer. Dover Publications Inc., New York

Cheong KB, Song TH (1997) An alternative discrete ordinates method with interpolation and source differencing for two-dimensional radiative transfer problems. Numer Heat Transfer B 32 (1):107-125

Chui EH, Raithby GD (1992) Implicit solution scheme to improve convergence rate in radiative transfer problems. Numer Heat Transfer B 22 (3):251-272

Coelho PJ (2002a) Bounded Skew High-Order Resolution Schemes for the Discrete Ordinates Method. J Comput Phys 175 (2):412-437

Coelho PJ (2002b) The role of ray effects and false scattering on the accuracy of the standard and modified discrete ordinates methods. J Quant Spectrosc Radiat Transfer 73:231-238

Coelho PJ (2004) A modified version of the discrete ordinates method for radiative heat transfer modelling. Comput Mech 33 (5):375-388

Coelho PJ (2005) A Hybrid Finite Volume/Finite Element Discretization Method for the Solution of the Solution of the Radiative Heat Transfer Equation. J Quant Spectrosc Radiat Transf 93 (1-3):89-101

Coelho PJ (2014) Advances in the discrete ordinates and finite volume methods for the solution of radiative heat transfer problems in participating media. J Quant Spectrosc Radiat Transfer 145 (0):121-146

Farmer JT, Howell JR (1994) Monte Carlo prediction of radiative heat transfer in inhomogeneous, anisotropic, nongray media. J Thermophys Heat Transfer 8 (1):133-139

Fiveland WA (1984) Discrete-ordinates solution of the radiative transport equation for rectangular enclosures. J Heat Transfer 106 (4):699-706

Fiveland WA (1988) Three-dimensional radiative heat-transfer solutions by the discrete-ordinates method. J Thermophys Heat Transfer 2 (4):309-316

Fiveland WA, Jessee JP (1994) Finite Element Formulation of the Discrete-ordinates Method for Multidimensional Geometries. J Thermophys Heat Transfer 8 (3):426-433

Fiveland WA, Jessee JP (1995) Comparison of discrete ordinates formulations for radiative heat transfer in multidimensional geometries. J Thermophys Heat Transfer 9 (1):47-54

Granate P, Coelho PJ, Roger M (2016) Radiative heat transfer in strongly forward scattering media using the discrete ordinates method. J Quant Spectrosc Radiat Transfer 172:110-120

Hou MF, Wu CY, Hong YB (2015) A closed-form solution of differential approximation for radiative transfer in a planar refractive medium. Int J Heat Mass Transfer 83:229-234

Howell JR (1968) Application of Monte Carlo to heat transfer problems. Adv Heat Transfer 5:1-54

Howell JR, Siegel R, Menguc MP (2011) Thermal radiation heat transfer. 5th edn. CRC Press, New York

Huang Y, Shi G-D, Zhu K-Y (2016) Runge–Kutta ray tracing technique for solving radiative heat transfer in a two-dimensional graded-index medium. J Quant Spectrosc Radiat Transfer 176:24-33

Huang Y, Xia XL, Tan HP (2002a) Radiative intensity solution and thermal emission analysis of a semitransparent medium layer with a sinusoidal refractive index. J Quant Spectrosc Radiat Transfer 74 (2):217-233
Huang Y, Xia XL, Tan HP (2002b) Temperature field of radiative equilibrium in a semitransparent slab with a linear refractive index and gray walls. J Quant Spectrosc Radiat Transfer 74 (2):249-261
Huang ZF, Zhou HC, Hsu P (2011) Improved discrete ordinates method for ray effects mitigation. J Heat Transfer 133 (4):044502
Hunter B, Guo Z (2012a) Conservation of asymmetry factor in phase function discretization for radiative transfer analysis in anisotropic scattering media. International Journal of Heat and Mass Transfer 55 (5):1544-1552
Hunter B, Guo Z (2012b) Phase-Function Normalization in the 3-D Discrete-Ordinates Solution of Radiative Transfer—PART II: Benchmark Comparisons. Numer Heat Transfer B 62 (4):223-242
Hunter B, Guo Z (2014) A new and simple technique to normalize the HG phase function for conserving scattered energy and asymmetry factor. Numer Heat Transfer B 65 (3):195-217
Hunter B, Guo Z (2015) Numerical smearing, ray effect, and angular false scattering in radiation transfer computation. Int J Heat Mass Transfer 81:63-74.
Klose AD, Netz U, Beuthan J, Hielscher AH (2002) Optical tomography using the time-independent equation of radiative transfer - Part 1: forward model. J Quant Spectrosc Radiat Transfer 72 (5):691-713
Koch R, Becker R (2004) Evaluation of quadrature schemes for the discrete ordinates method. J Quant Spectrosc Radiat Transfer 84 (4):423-435
Larsen EW, Thommes G, Klar A, Seaid M, Gotz T (2002) Simplified PN Approximations to the Equations of Radiative Heat Transfer and Applications. J Comput Phys 183 (2):652-675
Lathrop KD (1968) Ray effects in discrete ordinates equations. Nucl Sci Eng 32:357-369
Lemonnier D, Le Dez V (2002) Discrete ordinates solution of radiative transfer across a slab with variable refractive index. J Quant Spectrosc Radiat Transfer 73 (2-5):195-204
Li BW, Sun YS, Yu Y (2008) Iterative and direct Chebyshev collocation spectral methods for one-dimensional radiative heat transfer. Int J Heat Mass Transfer 51 (25-26):5887-5894
Li HS, Flamant G, Lu JD (2003) Mitigation of ray effects in the discrete ordinates method. Numer Heat Transfer B 43 (5):445-466
Liou KN (2002) An introduction to atmospheric radiation. Academic press, San Diego
Liu LH (2004a) Discrete curved ray-tracing method for radiative transfer in an absorbing-emitting semitransparent slab with variable spatial refractive index. J Quant Spectrosc Radiat Transfer 83 (2):223-228
Liu LH (2004b) Finite element simulation of radiative heat transfer in absorbing and scattering media. J Thermophys Heat Transfer 18 (4):555-557
Liu LH (2006) Finite volume method for radiation heat transfer in graded index medium. J Thermophys Heat Transfer 20 (1):59-66

Liu LH, Ruan LM, Tan HP (2002) On the discrete ordinates method for radiative heat transfer in anisotropically scattering media. Int J Heat Mass Transfer 45 (15):3259-3262

Liu LH, Tan HP (2006) Numerical simulation of radiative transfer in graded index media. Science Press, Beijing

Liu LH, Tan JY (2007) Least-squares collocation meshless approach for radiative heat transfer in absorbing and scattering media. J Quant Spectrosc Radiat Transfer 103 (3):545-557

Liu LH, Zhang L, Tan HP (2006) Radiative transfer equation for graded index medium in cylindrical and spherical coordinate systems. J Quant Spectrosc Radiat Transfer 97 (3):446-456

Liu LH, Zhao JM, Tan HP (2008) The finite element method and spectral element method for numerical simulation of radiative transfer equation. Science press, Beijing

Mahian O, Kianifar A, Kalogirou SA, Pop I, Wongwises S (2013) A review of the applications of nanofluids in solar energy. Int J Heat Mass Transfer 57 (2):582-594

Maruyama S (1993) Radiation Heat Transfer Between Arbitrary Three-Dimensional Bodies with Specular and Diffuse Surfaces. Numerical Heat Transfer, Part A: Applications 24 (2):181-196

Mengüç MP, Iyer RK (1988) Modeling of radiative transfer using multiple spherical harmonics approximations. J Quant Spectrosc Radiat Transfer 39 (6):445-461

Mengüç MP, Viskanta R (1985) Radiative transfer in three-dimensional rectangular enclosures containing inhomogeneous, anisotropically scattering media. J Quant Spectrosc Radiat Transfer 33 (6):533-549

Modest MF (2013) Radiative heat transfer. 3rd edn. Academic Press, New York

Modest MF, Haworth DC (2016) Radiative Heat Transfer in Turbulent Combustion Systems: Theory and Applications. Springer International Publishing, Cham

Murthy JY, Mathur SR (1998) Finite Volume Method for Radiative Heat Transfer Using Unstructured Meshes. J Thermophys Heat Transfer 12 (3):313-321

Pilon L, Berberoglu H, Kandilian R (2011) Radiation transfer in photobiological carbon dioxide fixation and fuel production by microalgae. J Quant Spectrosc Radiat Transfer 112 (17):2639-2660

Raithby GD, Chui EH (1990) A finite-volume method for predicting a radiant heat transfer in enclosures with participating media. J Heat Transfer 112:415-423

Ramankutty MA, Crosbie AL (1997) Modified discrete ordinates solution of radiative transfer in two-dimensional rectangular enclosures. J Quant Spectrosc Radiat Transfer 57 (11):107-140

Sadat H (2006) On the use of a meshless method for solving radiative transfer with the discrete ordinates formulations. J Quant Spectrosc Radiat Transfer 101 (2):263-268

Siegel R, Howell JR (2002) Thermal radiation heat transfer. 4th edn. Taylor and Francis, New York

Simmons FS (2000) Rocket exhaust plume phenomenology. Aerospace Corporation,

Song TH, Park CW Formulation and application of the second-order discrete ordinate method. In: Wang B-X (ed) Transport Phenomena and Science, 1992. Higher Education Press, pp 833-841

Sun YS, Li BW (2009) Chebyshev collocation spectral method for one-dimensional radiative heat transfer in graded index media. Int J Therm Sci 48:691-698

Tagne Kamdem HT (2015) Ray Effects Elimination in Discrete Ordinates and Finite Volume Methods. J Thermophys Heat Transfer 29 (2):306-318

Thurgood CP, Pollard A, Becker HA (1995) The TN Quadrature Set for the Discrete Ordinates Method. J Heat Transfer 117 (4):1068-1070

Truelove JS (1988) Three-dimensional radiation in absorbing-emitting-scattering media using discrete-ordinate approximation. J Quant Spectrosc Radiat Transfer 39 (1):27-31

Viskanta R, Mengüç MP (1987) Radiation heat transfer in combustion systems. Prog Energy Combust Sci 13 (2):97-160

W. An, L.M. Ruan, H. Qi, Liu LH (2005) Finite element method for radiative heat transfer in absorbing and anisotropic scattering media. J Quant Spectrosc Radiat Transfer 96 (3-4):409-422

Wang Z, Cheng Q, Wang G, Zhou H (2011) The DRESOR method for radiative heat transfer in a one-dimensional medium with variable refractive index. J Quant Spectrosc Radiat Transfer 112 (18):2835-2845

Wu CY, Hou MF (2012) Solution of integral equations of intensity moments for radiative transfer in an anisotropically scattering medium with a linear refractive index. Int J Heat Mass Transfer 55 (7–8):1863-1872

Xia XL, Huang Y, Tan HP (2002) Thermal emission and volumetric absorption of a graded index semitransparent medium layer. J Quant Spectrosc Radiat Transfer 74 (2):235-248

Zhang L, Zhao JM, Liu LH (2010) Finite Element Approach for Radiative Transfer in Multi-Layer Graded Index Cylindrical Medium with Fresnel Surfaces. J Quant Spectrosc Radiat Transfer 111 (3):420-432

Zhang L, Zhao JM, Liu LH (2016) A New Stabilized Finite Element Formulation for Solving Radiative Transfer Equation. J Heat Transfer 138 (6):064502-064502.

Zhang L, Zhao JM, Liu LH, Wang SY (2012) Hybrid finite volume/ finite element method for radiative heat transfer in graded index media. J Quant Spectrosc Radiat Transfer 113 (14):1826-1835

Zhang Y, Yi HL, Tan HP (2015) Analysis of transient radiative transfer in two-dimensional scattering graded index medium with diffuse energy pulse irradiation. Int J Therm Sci 87:187-198

Zhao JM, Liu LH (2006) Least-Squares Spectral Element Method for Radiative Heat Transfer in Semitransparent Media. Numer Heat Transfer B 50 (5):473-489

Zhao JM, Liu LH (2007a) Second Order Radiative Transfer Equation and Its Properties of Numerical Solution Using Finite Element Method. Numer Heat Transfer B 51:391-409

Zhao JM, Liu LH (2007b) Solution of Radiative Heat Transfer in Graded Index Media by Least Square Spectral Element Method. Int J Heat Mass Transfer 50:2634-2642

Zhao JM, Tan JY, Liu LH (2012a) A deficiency problem of the least squares finite element method for solving radiative transfer in strongly inhomogeneous media. J Quant Spectrosc Radiat Transfer 113 (12):1488-1502

Zhao JM, Tan JY, Liu LH (2012b) On the derivation of vector radiative transfer equation for polarized radiative transport in graded index media. J Quant Spectrosc Radiat Transfer 113 (3):239-250

Zhao JM, Tan JY, Liu LH (2013) A second order radiative transfer equation and its solution by meshless method with application to strongly inhomogeneous media. J Comput Phys 232 (1):431-455

Zhou HC, Cheng Q The DRESOR method for the solution of the radiative transfer equation in gray plane-parallel media. In: Mengüç MP, Selçuk N (eds) Proceedings of the Fourth International Symposium on Radiative Transfer, Istanbul, Turkey, 2004. pp 181-190

Zhou HC, Lou C, Cheng Q, Jiang Z, He J, Huang B, Pei Z, Lu C (2005) Experimental investigations on visualization of three-dimensional temperature distributions in a large-scale pulverized-coal-fired boiler furnace. Proc Combust Inst 30 (1):1699-1706

Zhu KY, Huang Y, Wang J (2011) Curved ray tracing method for one-dimensional radiative transfer in the linear-anisotropic scattering medium with graded index. J Quant Spectrosc Radiat Transfer 112 (3):377-383